

**POLITECNICO DI TORINO**

Collegio di Ingegneria Chimica e dei Materiali

**Corso di Laurea Magistrale  
in Ingegneria Chimica e dei Processi Sostenibili**

Tesi di Laurea Magistrale

**Synthesis and Characterization of  
nanostructured materials for indoor  
abatement**



**Relatore/i**

prof. Marco Piumetti  
prof. Samir Bensaid  
prof Nunzio Russo

**Candidato**

Ginevra Bonifazi

Dicembre 2023

## ABSTRACT

The following thesis aims to address the constantly looming problem of indoor pollution. Every year millions of people die due to the polluted air they breathe indoors. In fact, most of our time is spent in isolated environments where the air exchange is not so sudden. This situation causes the accumulation of molecules harmful to our respiratory and cardiovascular systems, leading to the onset of often lethal pathologies. The main consequences on human health are listed, as well as the molecules that are monitored to establish the air quality index (AQI). It then goes on to consider the state of the art and the technologies to date that are on the market or, still, under development. First, the laws and protocols used to design infrastructures such as offices, hospitals, and schools to ensure proper air circulation are mentioned. Among the various abatement techniques, we focus on thermal catalysis, which represents a fair compromise between performance, stability, and cost. Manganese oxides are indeed effective for abatement of substances such as volatile organic compounds (VOCs). In the experimental part of the thesis, the different aspects related to the morphology and chemical composition of the  $MnO_2$  and  $Mn_2O_3$  type catalysts synthesized by Solution Combustion Synthesis (SCS) technique are, therefore, analysed and compared with the respective commercial ones. This technique is advantageous as it is simple and hasty and allows you to obtain porous solids. We will note that the former,  $MnO_2$  SCS is characterized by better performance already under dry conditions. For this reason, subsequent tests will be conducted using only this type of catalyst. The molecules that are going to be used as pollutants are ethylene, propylene, and carbon monoxide. Tests under dry conditions were repeated 4 times for each pollutant to ensure reproducibility. The surface morphology, structure and chemical composition of the various samples are to be determined through characterization techniques of the XPS, XRD,  $H_2$ -TPR,  $O_2$ -TPD, FESEM and physisorption with nitrogen at  $-196^\circ\text{C}$ . Next, we move on to the actual testing phase in which we aim to determine the abatement capacity in the presence and absence of moisture and in which we go on to consider the stability of the catalyst by Time on Stream (TOS) and cyclic tests. Lastly, tests were also carried out to prove the reproducibility of the experiments carried out. These tests consisted of the conversion of ethylene propylene or carbon monoxide with a concentration of 100 ppm, 21% oxygen and nitrogen to balance. The aim was to try to simulate an indoor polluted air condition. Humidity in wet tests was estimated at 10%. The operating temperature range has always been between 25 and  $300^\circ\text{C}$  in order not to damage the catalyst by getting too close to the calcination temperature of  $650^\circ\text{C}$ . Through the characterizations it was possible to find that  $MnO_2$  SCS is better than the other samples analysed. Its surface area is around  $35\text{ m}^2/\text{g}$ , determining a rate for the conversion of ethylene equal to  $33,4\text{ mol/h/g}$ . For this reason, tests in the presence of humidity or to study stability were conducted on this catalyst, that proved to be the best performing. Finally, considerations will be made to correlate the chemical and physical properties of the catalyst with its activity and stability.

# Sommario

I Introduzione	4
I.I Obbiettivi	6
II Caratterizzazioni risultati	8
II.I Fisisorbimento in N <sub>2</sub>	8
II.II Diffrazione raggi X	10
II.III Elettro fotometria a raggi X	11
II.IV Microscopia a scansione	12
II.V Riduzione a temperatura programmata	13
II.VI Ossidazione a temperatura programmata	14
II.VII FESEM	14
III Impostazione dei Test	14
III.I Test in condizioni secche	15
III.II Test in condizioni umide	17
IV Risultati test	18
IV.I Test in condizioni secche a scalino	18
IV.II Test in condizioni umide a scalino	19
IV.IV Test TOS	19
IV.V Test di riproducibilità	19
IV Conclusioni	20

# I Introduzione

La crescita esponenziale dei centri abitati e dei siti industriali e la conseguente migrazione di persone verso le grandi città ha determinato un aumento dell'inquinamento dei centri abitati. Questo fenomeno, che prende il nome di terziarizzazione, ha provocato un danno profondo alle condizioni sanitarie e ambientali in cui ognuno di noi vive, in particolare nei paesi che sono ancora in fase di sviluppo. Per quanto riguarda l'inquinamento indoor, i dati fanno sobbalzare: il WHO conta circa nove milioni di morti annuali dovute a una esposizione prolungata nel tempo ad aria inquinata da molecole tossiche e cancerogene, come la formaldeide e il benzene. I gas esausti delle macchine, il fumo di sigaretta, i prodotti che quotidianamente ognuno di noi usa per la cura della propria abitazione e del corpo emettono sostanze che contaminano l'aria. Un'attenzione crescente viene riservata al monitoraggio e allo studio della composizione dell'aria che si trova all'interno delle abitazioni e degli uffici. Le statistiche riportano che un individuo medio passa all'interno di luoghi chiusi circa il 90% del suo tempo giornaliero. (Sundell, 2004) Le sostanze presenti nell'aria, pur essendo in concentrazioni estremamente basse (si parla dell'ordine dei ppm), hanno un innegabile effetto sul lungo termine. Inoltre, vi è una differenza profonda fra l'aria definita outdoor e quella indoor. Quella esterna, infatti, per quanto anche essa ricca di inquinanti, ha la possibilità di circolare liberamente e di diluirsi limitando gli effetti dannosi. All'interno di un edificio, ancora di più all'interno di una stanza, il ricambio di aria non è altrettanto repentino, causando l'accumulo di sostanze tossiche. A livello tecnico, infatti, si deve distinguere l'inquinamento outdoor da quello indoor. La composizione dell'aria indoor risulta, secondo numerosi studi scientifici, più eterogenea di quella outdoor. Questo è dovuto alla presenza di innumerevoli fonti di contaminazione e la mancanza di un sistema di circolazione dell'aria efficiente. Noi stessi, ad esempio, se l'aria è inquinata, percepiamo, dopo tante ore passate all'interno di una stanza, la sensazione di mal di testa o nausea. In campo medico questo fenomeno viene definito SBS (sick building syndrome) ovvero sindrome da edificio malato. Sul breve termine questo provoca un malessere generale, ma sul lungo periodo, invece, è l'origine di numerose disabilità sensoriali e di gravi patologie respiratorie e cardiovascolari, spesso letali. Uno studio condotto da Woods e i suoi collaboratori nel 1987 sosteneva la fragile condizione di chi si trovava a lavorare all'interno di uffici. Infatti, la presenza di dispositivi come stampanti, scrivanie, sistemi di condizionamento scarsamente puliti o con filtri ormai saturi sono la fonte di innumerevoli inquinanti di tipo organico e biologico. (EPA-452/F-03-022)

Analizziamo in dettaglio i singoli aspetti di questa trattazione, cominciando con il definire attentamente che cosa si intende per ambiente chiuso. Secondo l'accordo del 27/09/2001 tra il Ministero della salute, le regioni e le province autonome, con il termine "ambienti indoor" ci si

riferisce a tutti quei luoghi che sono, in qualche modo, isolati dall'esterno. In tali luoghi vengono svolte numerose delle attività quotidiane e lavorative. (UNI EN ISO159, 2003) Specificatamente, quindi, si intendono le abitazioni, gli uffici pubblici e privati, le strutture comunitarie (come ospedali, scuole, caserme, banche), locali destinati a attività ricreative o sociali, e anche i mezzi di trasporto pubblici o privati (come auto, treno, aereo, nave etc.). In questa classe ricadono, quindi, tutti quei luoghi dove comunemente viene trascorsa la maggior parte del nostro tempo e il rischio di potenziali sorgenti di inquinamento è evidentemente elevato.

Le fonti dell'inquinamento indoor possono essere generalmente classificate come interne o esterne. Con fonti esterne ci si riferisce a tutti gli agenti inquinanti che, sospesi in aria o intrappolati all'interno di materiali, migrano nei nostri edifici; fra questi citiamo le particelle di smog, la polvere, il polline. Ciò nonostante, essi rappresentano solo una parte limitata degli inquinanti potenzialmente presenti in un ambiente indoor: giocano un ruolo cruciale, invece, le fonti di contaminazione interna. Molte nostre quotidiane abitudini come fumare, lavare, cucinare, o l'uso di determinate vernici ci espongono in modo continuativo a un'aria ricca di sostanze volatili.

Gli inquinanti possono essere classificati in differenti modi e una particolare classe, su cui ci soffermeremo nel corso della trattazione, sono i COV, composti organici volatili. Denominati tali per la loro elevata tensione di vapore, sono considerati dannosi alla salute umana. In questa tesi verranno trattate tre molecole in particolare, propilene, etilene e monossido di carbonio. La ragione di tale scelta ricade nella loro comune presenza in numerosi ambienti indoor. La loro origine può essere di diverso tipo: normali azioni di routine come spruzzarsi un deodorante, alla combustione di apparecchi elettrici in scarsità di ossigeno o dovuti a fenomeni di deterioramento di cibi come frutta o verdura.

La domanda che ci poniamo è quindi: come possiamo ridurre i danni? A livello europeo vengono attuati stringenti controlli sulla qualità dell'aria. Esistono due metodologie che hanno lo scopo di sottrarre queste molecole dall'aria che viene respirata: adsorbimento e abbattimento catalitico.

Molte di queste non vengono attualmente utilizzate a livello commerciale, ma solo studiate a livello sperimentale, altre invece sono largamente diffuse. Si deve comunque trovare un compromesso fra qualità della performance e costo del prodotto. La catalisi ossidativa a bassa temperatura è una tecnica che presenta elevate performance a costi moderati. La scelta determinante risiede nel tipo di catalizzatore utilizzato: generalmente i catalizzatori impiegati sono a base di ossidi di metalli di transizione come il manganese. Questi elementi rappresentano un'ottima alternativa all'uso di catalizzatori addizionati con metalli nobili in quanto risultano più resistenti a eventuali contaminanti presenti nella corrente gassosa da depurare e all'azione del tempo. (Arvind Varma, 2016) Ad oggi molte ricerche scientifiche sono infatti improntate sullo studio di ossidi metallici sempre più performanti. Nella sezione successiva si analizzano gli obiettivi di questo lavoro sperimentale.

## I.II Obiettivi

La seguente tesi ha lo scopo di introdurre il problema dell'inquinamento indoor. In particolare, ci si sofferma sulle fonti di questi contaminanti e le loro conseguenze sulla salute umana, le normative che definiscono il monitoraggio e i limiti di concentrazione e la progettazione degli edifici. Vengono considerati con particolare attenzione i composti organici volatili (COV), sia quelli che più comunemente vengono riscontrati in aria, sia quelli che verranno utilizzati per l'analisi sperimentale ovvero etilene, propilene. La terza molecola utilizzata è il monossido di carbonio, la cui origine è da ricercare in processi di combustione in mancanza di ossigeno sufficiente come stufe elettriche malfunzionanti o cucine a gas con un basso livello di ricircolo dell'aria. Verranno poi descritte le tecniche utilizzate correntemente per adsorbire o abbattere queste sostanze volatili concentrandosi sulla catalisi ossidativa a bassa temperatura e sul ruolo che hanno i catalizzatori a base di ossidi metallici. In particolare, un metallo di transizione che possiede ottime caratteristiche per quanto riguarda le sue performance catalitiche è il manganese. Per questo motivo all'interno della parte sperimentale vengono studiati due fasi cristalline  $MnO_2$  e  $Mn_2O_3$  sintetizzati con tecnica solution combustion synthesis (SCS) confrontandoli con i relativi commerciali.

La parte sperimentale viene divisa in sintesi, caratterizzazione, test catalitici e conclusioni dove si analizzeranno i risultati ottenuti. Le tecniche di caratterizzazione mirano a determinare in maniera quantitativa e qualitativa la morfologia, la struttura e la composizione della polvere. In particolare, sono state utilizzate il fisisorbimento con azoto a  $-196^\circ\text{C}$ , la diffrazione a raggi X (XRD), e la spettrofotometria a raggi X (XPS), il desorbimento di ossigeno a temperatura programmata  $O_2$ -TPD, e la riduzione con idrogeno a temperatura programmata  $H_2$ -TPR, e infine la microscopia a scansione elettronica (FESEM). I test catalitici svolti permettono di determinare la attività e la stabilità dei campioni. Inizialmente i primi test condotti sono in condizioni secche, ovvero in assenza di umidità. Questi permettono di comprendere fin da subito quale, fra i vari campioni considerati, sia il migliore a livello di performance. I test successivi, che sono più complessi, sono condotti solo per il campione che ha dimostrato di essere migliore dei rimanenti e riguardano: I test in condizioni di umidità, i test per lo studio della stabilità, time on stream e ciclici, e i test di riproducibilità. Per quanto riguarda le condizioni operative, la corrente entrante nel reattore ha una concentrazione di inquinante pari a 100 ppm, 21%<sub>vol</sub> di  $O_2$  e azoto a bilanciare, arrivando a una portata totale di 50 ml/min. L'obiettivo è ottenere delle conversioni complete, per tutte e tre le molecole campione mantenendoci in condizioni di basse temperature. Successivamente si cerca di capire quanto il catalizzatore più performante sia stabile nel tempo sia in presenza che in assenza di acqua. Infine, tramite i tests di riproducibilità sarà possibile capire se i risultati ottenuti possono essere ripetuti da operatori diversi, in momenti diversi, garantendo la possibilità di continuare la ricerca.

## **II Caratterizzazione dei catalizzatori risultati**

Le proprietà chimico-fisiche e meccaniche di un qualunque tipo di materiale sono strettamente legate alla morfologia, composizione e alla struttura che presenta e conoscerle ci permette, di prevedere determinati comportamenti o di poterli correlare con le performance catalitiche. Inoltre, ci permette di andare a sviluppare, in un secondo momento, tecniche più sofisticate finalizzate all'ottenimento di materiali più performanti e specifici per determinati tipologie di processi. Al fine di studiare i catalizzatori a base di ossido di manganese di tipo commerciale sintetizzati con tecnica SCS, sono state utilizzate le seguenti tecniche di caratterizzazione: fisisorbimento di azoto a  $-196^{\circ}\text{C}$ , diffrattometria a raggi X, fotoelettroroscopia a raggi X, riduzione e ossidazione a temperatura programmata e microscopia a scansione. La diffrattometria a raggi X (XRD) permette di indagare la struttura cristallina e la microstruttura analizzando il pattern di diffrazione. L'analisi spettroscopia fotoelettronica a raggi X (XPS) invece, viene sfruttata per l'analisi della composizione degli strati più superficiali del campione e l'eventuale presenza di contaminazione. Il fisisorbimento di un determinato gas sonda, in questo caso azoto, ci permette di appurare il livello di porosità del materiale. Inoltre, ci permette di analizzare la geometria e la dimensione del poro che viene ulteriormente confermata dalle immagini del campione ottenibili tramite il FESEM. Infine, le analisi di desorbimento e riduzione a temperatura programma in presenza di ossigeno e idrogeno rispettivamente permettono di capire che tipo di ossigeni sono presenti sulla superficie del catalizzatore ed esaminare la loro mobilità e quanto il materiale possa considerarsi riducibile.

### **II.I Fisisorbimento di azoto a $-196^{\circ}\text{C}$**

Al fine di analizzare la area superficiale, la struttura del poro dei campioni di  $\text{MnO}_2$  e  $\text{Mn}_2\text{O}_3$  commerciale e SCS è stato attuato un processo di fisisorbimento con azoto a  $-196^{\circ}\text{C}$ , in un secondo momento i dati sono stati processati, secondo il metodo di Brauner Emmett Teller (BET). Le due immagini sottostanti riportano le isoterme di adsorbimento e desorbimento. Da un'analisi di tipo qualitativo, possiamo già ottenere delle informazioni sulla natura del materiale considerato. Dai dati in letteratura, si può affermare che questi due materiali sono di natura mesoporosa, in quanto le isoterme presentano il fenomeno di isteresi. Come possiamo vedere dalla figura 5.1, la curva di desorbimento non corrisponde a quella di adsorbimento: durante l'adsorbimento, le molecole di gas cominciano a riempire il poro, formando un primo strato. Con il passare del tempo e l'aumento della pressione parziale, si sviluppano strati di azoto sempre più fitti. Questo porta a una instabilità della fase gas che, quindi, pur essendo a una pressione inferiore a quella di saturazione, condensa. Secondo la IUPAC, esiste poi una seconda distinzione, basata sulla forma delle isoterme. La forma di isoterma

è caratteristica dei materiali mesoporosi, In figura 5.1, sono riportati i grafici dei campioni di tipo SCS e commerciale. Il grafico (a), che si riferisce ai campioni commerciali, riporta una isteresi che suggerisce la presenza di pori interstiziali causati dalla presenza di aggregati di particelle a foglietti. La quantità di azoto adsorbita è nettamente inferiore rispetto al grafico (b) che fa riferimento ai campioni sintetizzati con tecnica SCS. (K. S. W. SING (UK & al., 1982)

Il grafico (b), che invece corrisponde a  $MnO_2$  e  $Mn_2O_3$  SCS, corrisponde al fenomeno di condensazione capillare all'interno di pori interstiziali prodotti dalla aggregazione di particelle. Questo ci dà un'idea, benché di tipo qualitativo, della capacità di adsorbimento delle due tipologie di materiali considerati. I due catalizzatori commerciali hanno una capacità di adsorbimento delle molecole di azoto nettamente inferiore rispetto alle medesime fasi cristalline sintetizzate con la tecnica SCS.

L'area superficiale è un parametro da considerare in quanto direttamente correlata alla porosità del nostro materiale, insieme ad altre grandezze come il volume specifico e la distribuzione della dimensione dei pori (pore size distribution). Essa è fondamentale per garantire una determinata attività superficiale. L'area specifica è definita come il rapporto fra la superficie totale del campione e la sua massa. A livello pratico una stima di questa area totale può essere ottenuta considerando la quantità di azoto che va a formare il primo layer.

Dalla tabella 1 riportata sotto si può notare che l'area superficiale è di un ordine di grandezza superiore per gli ossidi di manganese sintetizzati con tecnica SCS, in particolare  $MnO_2$  SCS presenta il valore più alto di  $35,7 \text{ m}^2/\text{g}$ , a seguire il  $Mn_2O_3$  SCS e quelli commerciali.

Per quanto riguarda il volume totale dei pori, notiamo che i valori sono, per i campioni SCS, 100 volte maggiori rispetto ai commerciali.

**Tabella I** Fisisorbimento con azoto con metodo BET risultati dell'area specifica

<b>Fisisorbimento di <math>N_2</math></b>	<b><math>Mn_2O_3</math> comm</b>	<b><math>Mn_2O_3</math> SCS</b>	<b><math>MnO_2</math> comm</b>	<b><math>MnO_2</math> SCS</b>
<b>Area specifica (<math>m^2/g</math>)</b>	1,6	20,1	0,4	35,7
<b>Volume totale pori (<math>cm^3/g</math>)</b>	0.007	0,075281	0,002	0,1
<b>Diametro medio pori (nm)</b>	20,3	14,5	23,2	12,8

Per quanto riguarda, invece la dimensione dei pori, il valore del volume viene ricavato considerando la quantità totale di azoto adsorbito. In generale un materiale può essere classificato come micro, meso e macro a seconda del diametro dei pori. Tutti e quattro i campioni considerati vengono



considerati come mesoporosi: il loro diametro medio è compreso fra 2 e 50 nm, in particolare i catalizzatori sintetizzati con tecnica SCS sono di valore inferiore.

Un'altra informazione che possiamo ricavare è la larghezza media dei pori. Dalla distribuzione della dimensione dei pori, figura 5.2, ottenuto tramite il metodo BJH, possiamo vedere che per  $\text{MnO}_2$  commerciale il massimo si attesta intorno ai 4 nm, mentre nel caso del SCS la distribuzione presenta un ulteriore picco a 17 nm per il  $\text{MnO}_2$ . Mentre per  $\text{Mn}_2\text{O}_3$ .

### II.III Diffrazione a raggi X (XRD)

La diffrazione a raggi X (XRD) è una caratterizzazione che va a determinare la struttura del campione in maniera non distruttiva. Ci serve per capire se sono presenti delle transizioni di fase o delle possibili direzioni preferenziali di crescita. In base alla forma del diffrattogramma ottenuto è possibile risalire alla tipologia di materiale che stiamo analizzando. Tramite i pattern si ottengono tre informazioni principali: profilo dei picchi, intensità dei picchi e posizione angolare. Il profilo e l'intensità ci permettono di considerare la orientazione preferenziale, la struttura e l'abbondanza di fasi specifiche. Il profilo, invece, è di essenziale importanza per analizzare il livello di cristallinità, e disordine del campione. Tramite l'uso del software High Score Plus, è stato possibile correlare il pattern con uno specifico tipo di materiale e alla sua fase. Dalla figura 5.4, notiamo che per  $\text{MnO}_2$  SCS e commerciale i picchi della diffrazione corrispondono, per entrambi i campioni, a quelli di una struttura di tipo tetragonale. Si tratta della Pirolusite ovvero diossido di manganese (IV) di tipo  $\beta$ . La pirolusite è un minerale facente parte del gruppo rutilo. Per entrambe le fasi cristalline il diffrattogramma del commerciale risulta chiaramente più definito in quanto la struttura è perfettamente cristallina, a differenza di quello sintetizzato con tecnica SCS. Il grado di purezza risulta essere del 100% in quanto non sono presenti picchi riscontrabili di altre tipologie di materiali. Per quanto riguarda invece,  $\text{Mn}_2\text{O}_3$  sia di tipo SCS che commerciale, sono Bixbiite C con struttura cristallografica di tipo cubico, anche definita come  $\text{Mn}_2\text{O}_3$  di tipo  $\alpha$ . Anche in questo caso, si nota come il commerciale posseda una struttura più cristallina e ordinata rispetto al corrispettivo sintetizzato con tecnica SCS. Il grado di purezza è del 100%. In figura 5.3 sono riportate le immagini che fanno riferimento ai modelli CAD delle strutture cristalline  $\text{MnO}_2 \beta$  e  $\text{Mn}_2\text{O}_3$  di tipo  $\alpha$ .

Consideriamo adesso una seconda informazione ottenibile tramite la diffrattometria a raggi X: i cristalliti. Il grano cristallino, o cristallita è una caratteristica struttura o orientazione del cristallo comune a certa porzione della polvere, e la dimensione e l'orientamento di questi è direttamente correlata al metodo di sintesi e alla storia termica del materiale. Una stima della dimensione dei cristalliti è stata ottenuta tramite l'utilizzo della equazione di Scherrer. Essa permette di correlare la

dimensione dei domini cristallini sub-micrometrici alla larghezza del picco di diffrazione (FWHM). Come possiamo notare in tabella 2, i cristalliti del campione MnO<sub>2</sub> SCS sono più piccoli rispetto agli altri. Una minor dimensione dei cristalliti indica che più spesso viene a mancare l'ordine del reticolo cristallino e di conseguenza esso presenta una maggiore quantità di difetti reticolari. Questi difetti influenzano profondamente le proprietà fisiche e meccaniche del materiale. Nel caso specifico dei catalizzatori, una maggiore presenza di difetti è una qualità ricercata in quanto determina una maggiore attività del materiale.

**Tabella II** dimensione dei cristalliti nm

<b>Dimensione dei cristalliti (nm)</b>	
MnO <sub>2</sub> SCS	7
MnO <sub>2</sub> commerciale	153
Mn <sub>2</sub> O <sub>3</sub> SCS	37
Mn <sub>2</sub> O <sub>3</sub> commerciale	136

## II.IV Spettroscopia fotoelettronica a raggi X (XPS)

La spettroscopia fotoelettronica a raggi X (X-ray photoelectron spectroscopy) permette di determinare le specie chimiche presenti sulla superficie del campione e il loro stato di ossidazione tramite l'iterazione della radiazione con la materia. Tale tecnica sfrutta i raggi X che hanno un'energia compresa fra i 200 e i 2000 eV, questi bombardano la superficie del materiale e viene conseguentemente misurata la energia cinetica emessa dagli elettroni. Si tratta di una tecnica particolarmente sensibile (circa 10 nm), capace di rilevare il numero di ossidazione degli elementi. È in grado di rilevare tutti gli elementi chimici ad eccezione di elio e idrogeno. In figura 5.4 sono riportate le deconvoluzione degli spettri di O1s e Mn2p dei campioni di MnO<sub>2</sub> e Mn<sub>2</sub>O<sub>3</sub> SCS e commerciale. Sulla superficie del catalizzatore sono presenti due specie di ossigeni, generalmente, gli  $\alpha$  e i  $\beta$ . I primi sono solo chemisorbiti, ovvero hanno formato un legame più o meno stabile con la molecola di metallo e di conseguenza hanno una discreta mobilità si tratta di specie come CO<sub>3</sub>-O<sub>2</sub>- e OH-. I secondi, invece, rientrano a far parte del reticolo cristallino vero e proprio e non sono altrettanto disponibili a partecipare a determinate reazioni di ossidazione. Inoltre, gli  $O_\alpha$  più elettrofili dei  $O_\beta$  e danno origine a reazioni di ossidazione completa con gli elementi con cui entrano in contatto, mentre quelli a  $O_\beta$  sono fonte di reazioni più selettive. Sono caratterizzati da un diverso livello di energia di legame e questo rende possibile un loro riconoscimento. Una stima del loro rapporto è essenziale per andare a valutare l'attività del materiale. Una maggiore presenza di ossigeni  $O_\alpha$  rende il materiale più attivo e capace di convertire più velocemente le molecole con cui viene a contatto.

In generale si può affermare che il segnale compreso fra i 529,7-530, 1eV fa riferimento a  $O_{\beta}$  ( $O^{2-}$ ). Invece, il segnale 531.1-531.7 eV si riferisce agli ossigeni  $O_{\alpha}$ . (Kaushik Natarajan, 2018)  
 In tabella 3 sono riportati i rapporti di  $O_{\alpha}/O_{\beta}$ . Come possiamo notare confrontando i valori percentuali di  $O_{\alpha}/O_{\beta}$  per  $MnO_2$  SCS rispetto al commerciale abbiamo una maggiore presenza di  $O_{\alpha}$ . Lo stesso vale per  $Mn_2O_3$ .

**Tabella III** rapporto di  $O_{\alpha}/O_{\beta}$

$MnO_2$ SCS	53%
$MnO_2$ comm	40%
$Mn_2O_3$ SCS	33%
$Mn_2O_3$ comm	21%

Per quanto riguarda invece lo spettro di  $Mn2p$  questo viene generalmente diviso in due sezioni  $Mn2p_{1/2}$  e  $Mn2p_{3/2}$ . Sulla superficie di un ossido a base di manganese possono essere presenti tre tipologie di ioni, dipendenti dal loro stato di ossidazione:  $Mn^{2+}$ ,  $Mn^{3+}$ ,  $Mn^{4+}$ , le cui energie di legame sono comprese nel range 641-643 eV. In generale una maggiore quantità di ioni  $Mn^{4+}$  determina un effetto positivo del campione in quanto avrà una maggiore tendenza a ridursi a basse temperature, rispetto agli altri ioni. (Deng, 2016)

I siti  $Mn^{2+}$  sono di forma tetraedrica mentre quelli  $Mn^{3+}$  sono di tipo ottaedrico. (Alain Manceau, 1992). In particolare,  $Mn^{2+}$  ha una energia di legame che si attesta intorno ai 640,5 e i 640,8 eV,  $Mn^{3+}$  fra 641,9 e 642,1 eV e  $Mn^{4+}$  fra 643,3 e 643,8 eV.

In tabella 4 sono riportati i valori percentuali dei vari ioni  $Mn^{2+}$ ,  $Mn^{3+}$ ,  $Mn^{4+}$  con le relative energie di legame. Si nota come  $MnO_2$  SCS presenti sulla superficie la maggiore percentuale di ioni  $Mn^{4+}$  rispetto ai restanti campioni.

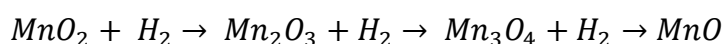
**Tabella IV** ioni manganese +2, +3,+4 e relativi rapporti

	BE	$Mn^{2+}$	BE	$Mn^{3+}$	BE	$Mn^{4+}$	$Mn^{4+}/$ $Mn^{3+}$	$Mn^{3+}/$ $Mn^{2+}$
$Mn_2O_3$ comm	640,8	76,3	641,5	17	643,3	7,7	0,41	0,22
$Mn_2O_3$ SCS	641,7	73,2	642,1	20,8	643,5	6	0,29	0,28
$MnO_2$ comm	641,5	89,6	642,5	14	643,4	6,4	0,40	0,16
$MnO_2$ SCS	641,1	49,4	642,5	35	643,3	15,6	0,45	0,61

## II.V Riduzione a temperatura programmata con idrogeno ( $H_2$ -TPR)

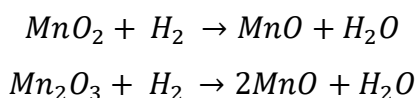
L'obiettivo è ottenere un consumo di idrogeno definito come [ $mmol/g_{cat}$ ]. Attraverso un detector a conducibilità termica (TCD) è possibile ricondursi alla presenza di reazioni di riduzione. La temperatura del picco è caratteristica del materiale ed è correlata alla reattività delle specie presenti sulla superficie della polvere catalitica.

Dalla figura 5.6 possiamo osservare che entrambi gli ossidi di manganese presentano due picchi:  $MnO_2$  commerciale a temperature maggiori (360, 540°C) rispetto a quelle del SCS (310, 410°C). Il processo di riduzione del manganese può essere generalizzato nel seguente modo: (Katpteijin et al, 1994)



I primi picchi, quindi, attesterebbero la riduzione del diossido di manganese a triossido di manganese, passando quindi da uno stato di ossidazione +4 a uno stato di ossidazione +3, il secondo picco invece da +3 a +2.

Di seguito è riportata la tabella 5 con i consumi di idrogeno normalizzati rispetto alla massa di campione impiegato e le relative temperature dei picchi. Al fine di calcolare l'area delle curve è stato utilizzato il software di ORIGIN®. Questi consumi sperimentali vengono confrontati con quelli teorici ottenuti considerando come stadio finale di ossidazione MnO.



Il consumo teorico di  $MnO_2$ , il valore è pari a 11,5  $mmol/g_{cat}$ , mentre per  $Mn_2O_3$  è pari a 6,33  $mmol/g_{cat}$ . Questo dato è servito in fase di elaborazione per capire quale fra i vari campioni fosse il migliore. Più il consumo di idrogeno è elevato, migliore è la sua capacità riduttiva. Allo stesso tempo, si deve considerare la temperatura del picco: minore è la temperatura del picco maggiore è la attività del materiale a temperature più basse. Nella figura 5.6 sono riportati i profili della TCD in funzione della temperatura in (a) per i catalizzatori  $Mn_2O_3$  e in (b) per  $MnO_2$  sia SCS che commerciali (comm).

In (a) notiamo come  $Mn_2O_3$  commerciale presenti un solo picco a una temperatura di 510°C, con un on-set a circa 300°C, corrispondente a un graduale processo di riduzione da  $Mn^{3+}$  a  $Mn^{2+}$ . Mentre il tipo SCS presenta due picchi di cui uno asimmetrico a una temperatura compresa fra i 300°C per il primo e 400°C-500°C per il secondo. Per questo possiamo dire che SCS è migliore rispetto al tipo commerciale. Nel grafico (b) invece vediamo come il tipo  $MnO_2$  commerciale abbia due picchi come per  $MnO_2$  SCS ma a temperature superiori, in entrambi i casi i picchi si riferiscono alla riduzione da  $Mn^{4+}$  a  $Mn^{3+}$  e da  $Mn^{3+}$  a  $Mn^{2+}$ . In tabella 5 vediamo come il migliore, in termini di consumi e di range di temperatura, sia  $MnO_2$  SCS, il primo picco si attesta intorno ai 300°C

corrispondente alla riduzione di  $\text{MnO}_2$  a  $\text{Mn}_2\text{O}_3$  e il consumo di idrogeno totale è molto vicino a quello teorico. Il fatto che  $\text{MnO}_2$  SCS si riduca a temperature inferiori rispetto a  $\text{Mn}_2\text{O}_3$  SCS è confermato anche dai risultati di XPS. Il valore degli ioni  $\text{Mn}^{4+}$  presenti sulla superficie del campione è maggiore nel caso di  $\text{MnO}_2$  SCS rispetto a  $\text{Mn}_2\text{O}_3$  SCS.

$\text{Mn}_2\text{O}_3$  SCS e commerciale hanno un consumo di idrogeno superiore a quello teorico calcolato, questo ci porta a pensare che sulla superficie siano presenti sia gli ioni  $\text{Mn}^{4+}$  che  $\text{Mn}^{3+}$  e che tutte e due subiscano un processo di riduzione. (Clarissa Cocuzza, 2023) Il dato è confermato dai risultati della caratterizzazione XPS, in tabella 4.

**Table V** Consumi di idrogeno catalizzatori normalizzati con relative temperature di picco

<b>H<sub>2</sub>-TPR</b>	<b>Temperatura range picco (°C)</b>	<b>mmol/gcat</b>
<b>MnO<sub>2</sub> SCS</b>	300-310	8,2
	400-410	3,1
<b>MnO<sub>2</sub> comm</b>	350-400	0,4
	500-550	5,1
<b>Mn<sub>2</sub>O<sub>3</sub> SCS</b>	300-310	2,6
	400-410	2,5
	450-500	1,8
<b>Mn<sub>2</sub>O<sub>3</sub> comm</b>	500-550	8

## II.VI Desorbimento di ossigeno a temperatura programmata ( $\text{O}_2$ -TPD)

Al fine di analizzare la mobilità degli ossigeni presenti sulla superficie della polvere catalitica è stata utilizzata la tecnica  $\text{O}_2$ -TPD, il desorbimento a temperatura programmata di ossigeno.

Anche in questo caso, come per la TPR, è stato attuato un pretrattamento in corrente di elio con un flusso di 40 ml/min per 1 ora a una temperatura di 400 °C. Il processo di desorbimento invece prevedeva di arrivare a una temperatura di 850°C. Gli ossigeni del reticolo in letteratura vengono classificati come  $\alpha$ ,  $\beta$ ,  $\gamma$  a seconda della forza del legame ossigeno e manganese. In generale quando il manganese è caratterizzato da uno stato di ossidazione +4 allora gli ossigeni del reticolo sono classificati come di tipo  $\gamma$ . In generale osserviamo tre picchi di cui il primo particolarmente facile da riconoscere. Per il diossido di manganese commerciale il picco si trova a una temperatura di circa 600°C mentre per quello di tipo SCS a una temperatura minore di 525°C. Gli ossigeni del reticolo di  $\text{MnO}_2$  SCS possono essere considerati quindi più reattivi in quanto il legame risulta essere più labile. (V.P. Santos, 2010)

In figura 5.7 sono riportati i profili delle prove di  $\text{O}_2$ -TPD in funzione della temperatura. Si può notare come  $\text{MnO}_2$  SCS cominci a desorbire ossigeno a temperature inferiori rispetto al commerciale. La stessa osservazione vale per  $\text{Mn}_2\text{O}_3$  SCS, il cui primo picco di desorbimento di ossigeno attesta intorno ai 500°C.

La seguente tabella riporta i dati dell'ossigeno desorbito. Notiamo che  $MnO_2$  SCS desorbe la maggiore quantità di ossigeno rispetto a tutti gli altri campioni. Già a temperature intorno ai  $500^\circ C$  notiamo un desorbimento pari a  $0,6 \text{ mmol/g}_{cat}$ .

**Tabella VI** Dati di desorbimento specifico di ossigeno per i catalizzatori

<b>O<sub>2</sub>- TPD</b>	<b>Temperature range (<math>^\circ C</math>)</b>	<b><i>mmol/g<sub>cat</sub></i></b>
<b><i>MnO<sub>2</sub>SCS</i></b>	500-550	0,6
	>800	0,1
<b><i>MnO<sub>2</sub>comm</i></b>	600-650	0,6
	>800	0,2
<b><i>Mn<sub>2</sub>O<sub>3</sub> SCS</i></b>	500-550	0,1
	>800	0,2
<b><i>Mn<sub>2</sub>O<sub>3</sub> comm</i></b>	>800	0,2

## II.V FESEM

In figura 5.8 sono riportate le immagini ottenute con il microscopio a scansione. In figura 5.8 sono riportate le immagini delle superfici dei campioni di  $MnO_2$  e  $Mn_2O_3$  sintetizzati con tecnica SCS (a) e (b) rispettivamente. Come si può osservare la superficie del campione  $MnO_2$  SCS ha i cristalli di forma tetragonale come riscontrato dalla diffattometria a raggi X. In (b) invece si notano i cristalli di tipo cubico tipici di  $Mn_2O_3$  di tipo  $\alpha$ .

## III Test catalitici set up

### III.I Test in condizioni secche

Dopo aver analizzato, tramite le precedenti tecniche di caratterizzazione, le proprietà chimico fisiche dei campioni ottenuti, si passa ora a considerare le loro performance catalitiche. In questa tesi sono stati condotti differenti tipologie di tests con lo scopo di andare a determinare quale fra i quattro catalizzatori utilizzati fosse il più adatto ad abbattere le molecole campione. Innanzitutto, si considerano i test in condizioni secche, poi quelli in condizioni umide, quelli ciclici, i time-on-stream e quelli sulla riproducibilità. Attraverso l'utilizzo di un microreattore tubolare in Quartz-U a letto fisso è stata condotta un'ossidazione catalitica a temperature che non superassero mai i  $300^\circ C$ , volendo rimanere in condizioni di basse temperature. Per tutti i test svolti, anche i time-on stream e ciclici, è effettuato un pretrattamento in cui il catalizzatore viene lasciato all'interno del reattore per

un periodo di un'ora in azoto a una temperatura di 160°C al fine di rimuovere eventuali impurità adsorbite sulla superficie del catalizzatore. La corrente di azoto inviata al reattore era 100 ml/min. La miscela composta da 100 ppm del COV di interesse (propilene, etilene) o monossido di carbonio, 21% di ossigeno e azoto a bilanciare. L'apparato sperimentale, in figura 4.1, per i tests in condizioni secche era composto da tre macrosezioni che potremmo riassumere in: apparato preparazione miscela, sistema di riscaldamento con reattore e infine apparato di analisi dei reagenti e prodotti. In particolare, il forno, fatto con materiale isolante, conteneva al suo interno il tubo in quarzo, all'estremità del quale vi era una termocoppia. La massa di catalizzatore utilizzato è di 50 mg, rimasta fissa per tutte le tipologie di test. In questo caso, non essendo presenti analizzatori appositi per i VOC, ma soltanto per il monossido di carbonio e l'anidride carbonica, al fine di calcolare la conversione di etilene e propilene a CO<sub>2</sub> è stata utilizzata la seguente formula

$$\text{Conversione (\%)} = \frac{F_{CO_2}}{nF_{VOC,in}}(\%) \quad \text{equazione 1}$$

Dove i simboli rappresentano

$F_{CO_2}$  la portata di diossido di carbonio prodotta.

$n$ : numero di atomi di carbonio presenti nella molecola (etilene, propilene: 2,3)

$F_{VOC,in}$  la portata di inquinante in ingresso

Tutto ciò è stato possibile ipotizzando che la concentrazione di anidride carbonica in arrivo all'analizzatore fosse derivante dalla conversione della molecola di inquinante. Per quanto riguarda l'impostazione dei test, questa varia a seconda della tipologia. In generale, ogni test è preceduto da una fase di pretrattamento a 160°C per un'ora con 100 ml/min di azoto puro. I test possono essere con una crescita lineare della temperatura di 5°C al minuto e vengono definiti a rampa; nei test a scalino, invece, la temperatura viene aumentata di 25°C alla volta dopo che il sistema ha raggiunto lo stazionario.

In figura 4.1 è riportato il grafico dell'apparato sperimentale per i tests di tipo wet, che in aggiunta a quello precedente presenta due ulteriori parti: la prima che permette la miscelazione del vapore acqueo con la miscela di ossigeno e azoto e la seconda che, invece, permette di condensare l'acqua presente nella corrente uscente dal reattore. La fase di condensazione è estremamente importante per non andare a danneggiare l'analizzatore che, pur presentando all'entrata un filtro anti umidità, non può sopportare una concentrazione di acqua così elevata.

In questa fase dello studio, come nelle successive, è stato fatto uso esclusivamente del catalizzatore MnO<sub>2</sub> SCS in quanto ha dimostrato di convertire a temperature più basse le molecole di CO, etilene e propilene. Per i tests in condizioni umide, la procedura prevedeva che prima di ogni ciclo di conversione vi fosse una fase di pretrattamento, come per i test precedenti. In particolare, una corrente di azoto di bombola di 100ml/min è inviata all'interno reattore a una temperatura di 160°C per un'ora

circa. Dopo aver raffreddato il reattore e dopo aver preparato la miscela con 21% di ossigeno, 100ppm di inquinante e azoto a bilanciare si procede a chiudere il by-pass. Aveva quindi inizio il primo ciclo di conversione, al termine del quale si apriva il bypass e si diminuiva la temperatura. Di nuovo si ripartiva con il pretrattamento e così fino al terzo ciclo. Come per i precedenti test si registrava la temperatura e la concentrazione dell'anidride carbonica in uscita e tramite un bilancio si andava a stimare la conversione

## IV Risultati

### IV.I Tests catalitici in condizioni dry a scalino

La figura 6.1 riporta le conversioni in funzione della temperatura delle molecole di monossido di carbonio, etilene e propilene.

La molecola che risulta più difficile da convertire è l'etilene, in quanto a causa del legame doppio C-C è più difficile da adsorbire su un eventuale sito attivo. Di conseguenza, per poterla convertire, la temperatura raggiunta è maggiore. La molecola di monossido di carbonio, invece, nonostante presenti un triplo legame è più facile da degradare per la presenza di un legame fortemente polarizzato sull'ossigeno, essa quindi tende naturalmente a convertirsi in anidride carbonica a temperature di 125°C in presenza di MnO<sub>2</sub> SCS. Mentre per propilene ed etilene le temperature raggiunte, per la completa conversione, sono rispettivamente 175°C e 225°C.

Nella tabella 6 vengono riportate le velocità di conversione dei diversi catalizzatori alle temperature di 50°C per il monossido di carbonio, 125°C per l'etilene e 100°C per il propilene in modo da avere una conversione inferiore al 20%, ed essere in controllo cinetico. Si nota come i valori di velocità, normalizzati sulla massa di catalizzatore di 50 mg, siano di due ordini di grandezza superiori per i catalizzatori sintetizzati con tecnica SCS. Anche in questa situazione MnO<sub>2</sub> SCS risulta comunque il migliore per convertire le molecole inquinanti.

**Tabella VII** Rates normalizzate rispetto alla massa di catalizzatore il catalizzatore di Mn<sub>2</sub>O<sub>3</sub> e MnO<sub>2</sub> commerciale sono stati omessi perché non attivi alle temperature scelte

	Temperatura	Mn <sub>2</sub> O <sub>3</sub> SCS (nmol/h/m <sup>2</sup> )	Conversione	MnO <sub>2</sub> SCS (nmol/h/m <sup>2</sup> )	Conversione
<b>CO</b>	75°C	0,6	2%	6,2	31%
<b>Etilene</b>	125°C	2,8	12%	3	14%
<b>Propilene</b>	125°C	4,4	12%	7,1	36%



**Tabella VIII** T10, T50 e T90 dei catalizzatori  $\text{MnO}_2$  e  $\text{Mn}_2\text{O}_3$  commerciali e SCS

<b>Etilene</b>	<b><math>\text{Mn}_2\text{O}_3</math> SCS</b>	<b><math>\text{Mn}_2\text{O}_3</math> commerciale</b>	<b><math>\text{MnO}_2</math> SCS</b>	<b><math>\text{MnO}_2</math> commerciale</b>
<b>T<sub>10%</sub></b>	92	188	118	193
<b>T<sub>50%</sub></b>	227	227	131	265
<b>T<sub>90%</sub></b>	260	>300	282	>300

<b>Propilene</b>	<b><math>\text{Mn}_2\text{O}_3</math> SCS</b>	<b><math>\text{Mn}_2\text{O}_3</math> commerciale</b>	<b><math>\text{MnO}_2</math> SCS</b>	<b><math>\text{MnO}_2</math> commerciale</b>
<b>T<sub>10%</sub></b>	122	192	102	179
<b>T<sub>50%</sub></b>	174	270	134	224
<b>T<sub>90%</sub></b>	211	>300	164	268

<b>Monossido di carbonio</b>	<b><math>\text{Mn}_2\text{O}_3</math> SCS</b>	<b><math>\text{Mn}_2\text{O}_3</math> commerciale</b>	<b><math>\text{MnO}_2</math> SCS</b>	<b><math>\text{MnO}_2</math> commerciale</b>
<b>T<sub>10%</sub></b>	100	136	54	137
<b>T<sub>50%</sub></b>	140	189	84	184
<b>T<sub>90%</sub></b>	182	248	111	250

#### **IV.II Risultati test catalitici in condizioni umide (10% RH di H<sub>2</sub>O)**

Dai grafici riportati in figura 6.2 si può notare come la presenza di vapore acqueo all'interno della corrente da convertire provochi un effettivo abbassamento delle performance del catalizzatore. Questo è dovuto al fatto che nel momento in cui la miscela di inquinante incontra la superficie del catalizzatore, non solo le molecole di inquinante saranno interessate a un fenomeno di adsorbimento sul sito catalitico, ma anche le molecole di acqua che, però, non andando a reagire rappresenteranno solo un ostacolo fisico. In particolare la molecola di monossido di carbonio viene convertita completamente a 175°C, l'etilene a 250°C e il propilene a 225°C.

#### **IV.III Risultati test ciclici**

In figura 6.3, i grafici (a), (b), (c) delle molecole di monossido di carbonio, etilene e propilene. Le curve di conversione sono sovrapposte in tutti e tre i casi a riprova della stabilità del catalizzatore  $\text{MnO}_2$  SCS. Questo ci porta a dire che i siti attivi del campione di  $\text{MnO}_2$  SCS rimangono disponibili per tutti e tre i cicli di conversione senza essere danneggiati da fenomeni di sintering dovuti a un eccessivo utilizzo del materiale per la catalisi delle reazioni.

#### **IV.IV Risultati test Time on stream tests (TOS)**

I TOS sono svolti sia in presenza che in assenza di vapore acqueo. In condizioni secche, il test è stato svolto sia con catalizzatore fresco figura 6.4 sia dopo aver subito tre cicli di conversione, , figura 6.5. In figura 6.4 osserviamo la conversione con MnO<sub>2</sub> SCS fresco e la conversione rimane stabile per tutte e tre le molecole. In (a) osserviamo che la conversione si mantiene a un valore medio del 92,4% per tutte le otto ore. Per etilene e propilene, (b) e (c) rispettivamente, si assiste a un lieve calo della conversione dopo circa quattro ore per l'etilene e dopo due ore per il propilene. In particolare, nel caso dell'etilene la conversione diminuisce passando da un 90% circa a quasi 85%. Nel caso del propilene invece, si ha un picco al 90% per poi diminuire abbastanza repentinamente e stabilizzarsi a un valore medio del 80%. Questo fenomeno può essere correlato alla conseguente tappatura di alcuni siti attivi da parte delle molecole di inquinante o da parte delle molecole di CO<sub>2</sub> prodotte che non liberano il sito attivo una volta formate. In questo caso, quindi, sarebbe necessario un processo di rigenerazione ad alte temperature. Per quanto riguarda il catalizzatore non fresco di MnO<sub>2</sub> SCS. Come possiamo vedere dai grafici della figura 6.5 (a), (b), (c) che fanno riferimento alle molecole di CO, etilene e propilene, la conversione rimane stabile. Questi grafici, fanno riferimento a catalizzatori che avevano già subito tre cicli di conversione, quindi non si è potuto considerarli effettivamente freschi. In particolare, la conversione del monossido di carbonio rimane costante per tutte le otto ore a un valore di 83%. Per la molecola di etilene si è scelta una temperatura di 210° C, a cui corrispondeva una conversione di circa 94 %. Possiamo notare come il catalizzatore reagisca bene nelle prime quattro ore, mantenendo un andamento costante della conversione, e in seguito, si ha una lieve diminuzione e si scende a 87% di conversione circa. Per la molecola di propilene assistiamo a una lenta diminuzione della conversione che passa da 80% a inizio test a quasi 73% verso la fine. In figura 6.6, sono stati condotti dei tests di tipo TOS in condizioni di umidità relativa del 10%. In questo caso, al fine di mantenere la conversione prossima a un valore del 90% si è dovuto aumentare la temperatura operativa: 175°C per il monossido di carbonio, 240°C per etilene e 215°C per il propilene. Risultati ottimi sono stati ottenuti per il monossido di carbonio la cui conversione si mantiene stabile per tutta la durata del ciclo. Per le molecole di etilene e propilene invece si nota come la presenza di acqua infici sulla stabilità del catalizzatore nel convertire gli inquinanti a CO<sub>2</sub> si nota come la conversione oscilla intorno al 90% stabilizzandosi solo nell'ultima fase di test. Questo può essere dovuto al fatto che il sistema, in presenza di vapore acqueo, avesse bisogno di più tempo per raggiungere una fase di stazionario rispetto alle condizioni secche. Nonostante questo, non si assiste a un calo drastico delle performance, di conseguenza possiamo affermare che il catalizzatore è considerabile come stabile.

#### **IV.V Test di riproducibilità**

La riproducibilità coinvolge tutti i contributi dell'incertezza di una misura che riguardino operatori, materiali e apparecchiature. Essa è fondamentale in ambito sperimentale, in quanto permette, in un secondo momento, di ottenere misure simili da operatori differenti, in modo da approfondire le ricerche. Inoltre, permette di andare a stimare il valore dell'errore sperimentale per poterlo minimizzare il più possibile garantendo che le analisi non si basino su metodi soggettivi.

In figura 6.7 sono riportati i grafici di riproducibilità delle molecole di monossido di carbonio, etilene e propilene ripetuti per cinque volte. Le curve risultano sovrapposte, permettendoci di considerare i risultati ottenuti come riproducibili. Lo scostamento massimo riscontrato nelle percentuali di conversione è pari a  $\pm 5\%$ . In figura 6.8, la deviazione standard aumenta e raggiunge il suo massimo nei punti in cui abbiamo un maggiore mal condizionamento, ovvero nei punti in cui la reazione è influenzata in egual misura dal controllo cinetico e dal controllo diffusivo.

## V Conclusioni

La seguente tesi aveva come obiettivo lo studio dei catalizzatori a base di ossido di manganese in merito all'abbattimento di molecole tossiche presenti in ambiente indoor come monossido di carbonio, etilene e propilene.

Innanzitutto, gli ossidi di manganese sono risultati dei buoni catalizzatori per l'abbattimento di queste sostanze a temperature inferiori ai  $300^{\circ}\text{C}$ , in particolar modo  $\text{MnO}_2$  SCS. In particolare, una maggiore area specifica e una minore dimensione dei cristalliti permette di avere più siti attivi a disposizione per le reazioni di ossidazione. L'attività di  $\text{MnO}_2$  SCS in quanto ha una maggiore percentuale di ioni  $\text{Mn}^{4+}$  e di  $\text{O}_\alpha$  sulla superficie rispetto agli altri catalizzatori considerati.

La presenza di acqua inficia sulle prestazioni di  $\text{MnO}_2$  SCS e si assiste a un aumento della temperatura per avere una conversione totale.

Nei test di tipo ciclico non si è assistita a nessuna variazione della conversione. I test TOS condotti in assenza di acqua hanno dimostrato la stabilità del catalizzatore  $\text{MnO}_2$  SCS fresco. Mentre per quanto concerne il campione già utilizzato per i test ciclici, si è assistito a un leggero calo della conversione nelle ultime ore di test, per le molecole di etilene e propilene dovuto probabilmente a un fenomeno di tappatura di alcuni siti attivi. I TOS in presenza di umidità hanno fatto emergere come la presenza di vapore acqueo rallenti l'arrivo a una fase stazionaria di conversione. I dati possono essere considerati riproducibili grazie ai test svolti nell'ultima fase sperimentale.

In futuro si potrebbe cercare di approfondire la tematica legata ai fenomeni degradativi che influenzano in maniera preponderante le molecole idrocarburiche di etilene e propilene. Inoltre sarebbe interessante analizzare il comportamento del catalizzatore all'aumentare del numero dei cicli di reazione. Al fine di migliorare le performance del catalizzatore, sarebbe opportuno addizionarlo con un metallo nobile come oro o platino al fine di diminuire la temperatura di esercizio.

# Index

Sommario.....	3
I Introduzione.....	4
I.II Obbiettivi.....	6
II Caratterizzazione dei catalizzatori risultati .....	7
II.I Fisisorbimento di azoto a -196°C.....	7
II.III Diffrazione a raggi X (XRD).....	9
II.IV Spettroscopia fotoelettronica a raggi X (XPS).....	10
II.V Riduzione a temperatura programmata con idrogeno (H <sub>2</sub> -TPR) .....	11
II.VI Desorbimento di ossigeno a temperatura programmata (O <sub>2</sub> -TPD).....	13
III Test catalitici set up.....	14
III.I Test in condizioni secche.....	14
IV Risultati.....	16
IV.I Tests catalitici in condizioni dry a scalino.....	16
IV.II Risultati test catalitici in condizioni umide (10% RH di H <sub>2</sub> O).....	17
IV.III Risultati test ciclici.....	17
IV.IV Risultati test Time on stream tests (TOS).....	17
IV.V Test di riproducibilità.....	18
V Conclusioni.....	19
1 Introduction.....	22
1.1 Objectives.....	24
1.2 Indoor air pollutants .....	25
1.3 Consequences of indoor pollution.....	26
1.4 Italian regulations for VOC concentrations .....	28
2 State of the art .....	29
2.1 VOC abatement techniques.....	32
2.1.1 Adsorption.....	33
2.1.2 Photocatalytic oxidation (PCO) .....	34
2.1.3 Plasma catalysis for VOCs oxidation.....	35
2.1.4 Incineration or thermal combustion .....	35
2.1.5 Catalysis for VOCs abatement.....	36
2.1.6 Transition metal oxides catalyst.....	37
2.1.7 Manganese oxides catalysts .....	39
2.1.8 Theoretical basis for the synthesis .....	40
2.1.9 Solution Combustion Synthesis .....	40
3 Catalyst characterization methods.....	43

3.1 Nitrogen physisorption at -196°C .....	43
3.2 X-Ray diffraction (XRD) .....	45
3.3 X-ray Photoelectron Spectroscopy (XPS).....	47
3.4 FESEM.....	48
3.5 H <sub>2</sub> -TPR and O <sub>2</sub> -TPD .....	48
4 Set up of tests .....	50
4.1 Dry tests with step.....	50
4.2 Catalytic Tests.....	50
4.3 Dry tests with steps .....	50
4.4 Wet tests with steps.....	51
4.5 Cyclic tests .....	52
5 Characterization results.....	54
5.1 Nitrogen physisorption at -196°C .....	54
5.2 X-Ray diffraction (XRD) .....	56
5.3 Photoelectron spectroscopy with X ray(XPS).....	58
5.4 Programmed temperature reduction with hydrogen (H <sub>2</sub> -TPR) .....	60
5.5 Temperature programmed desorption of oxygen (O <sub>2</sub> -TPD).....	63
5.6 FESEM results .....	64
6 Tests Results.....	65
6.1 Dry tests results.....	65
6.2 Humid Tests .....	67
6.3 Tests on the catalytic performance in time .....	68
6.3.1 Cyclic tests .....	68
6.4 Test for replicability.....	72
6.4.1 Replicability and reproducibility.....	72
6.4.2 Tests results.....	73
7 Conclusions.....	75
List of images.....	76
List of tables.....	77
List of equations.....	77
Riferimenti .....	78
Appendix.....	80
List of formula.....	80
Acronyms List.....	82
Ringraziamenti .....	83

# 1 Introduction

The exponential growth of population centers and industrial sites and the resulting migration of people to cities has led to an increase in pollution. This has caused profound damage to the health and environmental conditions in which everyone lives, particularly in countries that are still developing. (Sundell, 2004) Nowadays, the World Health Organization (WHO) counts about nine million annual deaths due to long-term exposure to air polluted with toxic and carcinogenic molecules, such as formaldehyde and benzene., cigarette smoke, and the products that each of us use daily to care for our homes and bodies emit substances that contaminate the air. Increasing attention is being paid to monitoring and studying the composition of the air found inside homes, offices, schools, and hospitals: environments that are somehow insulated from the outer. This situation leads to the accumulation of several kinds of compounds that are toxic for our respiratory and circulatory apparatus. Statistics report that about 90 % of the time the average individual spends indoors; this suggests how important it is to ensure unimpeachable air quality. (Hannah Blair, 2023) In fact, the substances present, although in extremely low concentrations (we are talking on the order of ppm), still have an effect over the long term. Moreover, there is a difference about the air defined as outdoor from indoor. (Paul B. Tchounwou, 2021) The outdoor one, although also rich in pollutants and soot, has the possibility to circulate freely and to "dilute" the harmful effects over an area certainly larger than those of a building. The composition of indoor air is, according to numerous scientific studies, significantly more varied than that of outdoor air. (Europe, 1989) This is due to the presence of innumerable sources of contamination all enclosed within an isolated or semi-isolated environment. Indeed, we feel the need, after many hours spent inside a room, the feeling of headaches or nausea. Medically, this phenomenon is called SBS (sick building syndrome). In the short term this causes a feeling of unwell, exhausted, but in the long term it is the cause of numerous sensory disabilities and serious respiratory and cardiovascular diseases, as previously cited. A study conducted by Woods and his collaborators in 1987 supported the fragile condition of those who found themselves working inside offices. The presence of printer devices, and air conditioning systems that are poorly cleaned are the source of countless organic and inorganic pollutants. (Europe, 1989)

According to the agreement of 09/27/2001 between the Ministry of Health, regions and autonomous provinces, the term "indoor environments" refers to all those places that are in some way isolated from the outside and in which many of the daily and work activities are carried out. (159, 2003) Specifically, it is meant to include dwellings, public and private offices, community facilities (such

as hospitals, schools, barracks, banks), premises intended for recreational and social activities, and public or private transport (such as car, train, plane, ship etc.). Thus, this class includes all those places where most of our time is commonly spent and the risk of potential sources of pollution is evidently high.

Sources of indoor pollution can generally be classified as either indoor or outdoor. By external sources, we refer to all pollutants that, suspended in the air or trapped inside any kind of material, migrate into our buildings. Smog particles, dust, pollen thus have free access to our buildings. These represent only a limited part; sources of internal contamination play a crucial role. They turn out to be significantly more numerous and profoundly different in nature. There are three types of contaminants in the air: chemical, physical, and biological. Many of our daily habits such as smoking, washing, cooking, or the use of paints continuously expose us to air rich in volatile substances. Another crucial aspect is precisely the air conditioning system of the affected environment, which, if not cleaned and sanitized regularly, is bound to become a proliferating breeding ground for mould and fungi, which can potentially contaminate entire buildings. Stringent air quality controls are implemented worldwide. The Five-Year Plan of China guaranteed to reduce the emissions of toxic compound such as VOC by 10% at the end of 2020. At the European level, according to the 2006 protocol of Goteborg every country should behalf the emission of VOCs by the end of 2020 in comparison with the one of 2000. Hence this political commitment has gave the right push to the scientific research. the aim is to convert complex molecules such as benzene or toluene into as many simpler ones that are less harmful to human health. Over the years, research has made it possible to synthesize nanostructured materials capable of converting pollutants into simpler and less harmful molecules such as water and carbon dioxide working at temperatures below 300°C. Generally, the degradation of VOCs through catalysis at low temperatures uses two types of nanostructured materials: noble metal supported and metal oxide-based catalysts. (EPA's Terms of Environment Glossary)

The use of noble metals is not a feasible solution as they are frequently subject to poisoning phenomena, which is why scientific research has focused on the study of transition metals which, to date, represent a perfect solution, in terms of energy expenditure, material cost, performance and resistance over time. Even today, despite the great results obtained, due to the complexity of the molecules and the variety of mixtures present in an indoor environment it has not yet been possible to define a single and definitive solution. (Katpteijin et al, 1994)

As for instead pollutants, they can be classified in different ways, and one class, which we will focus on later in the discussion, are VOCs, volatile organic compounds, (with a boiling point below 260°C at 25°C and 1 atmosphere). Because of their toxicity, high diffusivity and volatility they are

considered as a crucial factor to air pollution and are regarded as particularly harmful to human health and eco-environment. Three molecules in particular, propylene, ethylene, and carbon monoxide, will be analysed. The reason for this choice falls on their common presence in many indoor environments. Their origin can be of different types: normal routine actions such as spraying deodorant, to the combustion of electrical appliances in oxygen shortage or due to the degradation process of fruit and vegetables. (Sundell, 2004)

There are countless VOC abatement technologies, each with advantages and disadvantages for example adsorption, biological degradation, thermal incineration, and thermal catalytic oxidation. Some of these are not yet on the market as they are still in the testing phase, for example the plasmacatalysis. Others, however, do not involve a real chemical reaction, but rather a physical adsorption. Despite being an exploited technology on the market, adsorption cannot be considered a definitive solution as the molecule could be released later. Furthermore, after a certain period the material needs to be replaced or regenerated. A trade-off must be found between quality of performance and cost of the product. In this thesis, thermal catalytic oxidation at low temperature in presence of different types of manganese oxide catalysts will be discussed. Indeed, it is essential the catalyst choice to guarantee activity at the right temperature and stability over the time. The Solution Combustion Synthesis (SCS), which is a frequently used method because of its practicality, it is used to synthesize the studied manganese oxides. Although it is characterized by a very simple and hasty protocol, it still allows to obtain solids with a high degree of surface area and good porosity: fundamental characteristics for a catalyst. (Satu Ojala, 2011)

## **1.1 Objectives**

The following thesis aims to introduce the problem of indoor pollution. We focus on the sources of these contaminants and their consequences on human health, regulations defining monitoring and concentration limits, and building design. Special attention is given to volatile organic compounds (VOCs), those most commonly encountered and also those that are used for experimental analysis i.e. ethylene, propylene. The techniques currently used to adsorb or break down these organic substances is described, focusing on thermal catalytic oxidation at low temperature and the role played by metal oxide catalysts and the importance of Manganese among them. Next, the SCS technique is briefly described. Then, the exploited characterization techniques are mentioned. In particular in this experimental work in order to study the obtained samples physisorption with nitrogen at  $-196^{\circ}\text{C}$ , X-ray diffraction XRD, and X-ray spectrophotometry (XPS), oxygen desorption at programmed temperature  $\text{O}_2$ -TPD, and reduction in the presence of hydrogen at programmed temperature  $\text{H}_2$ -TPR, and finally FESEM, a type of scanning electron microscopy, are



used. The experimental part is divided into summary, characterization, catalytic tests, and conclusions where the results obtained will be analysed. The studied catalysts are two different crystalline phases of manganese oxides:  $\text{MnO}_2$  and  $\text{Mn}_2\text{O}_3$  SCS, compared to relative commercials. Characterization techniques aim to determine the morphology, structure, and composition of the obtained powder.

The catalytic tests carried out allow to determine the activity and stability of the samples. Initially, the first tests conducted were in dry conditions, i.e. in the absence of humidity. These allow us to immediately understand which, among the various samples considered, is the best in terms of performance. Subsequent tests, which are more complex, are conducted only for the sample that proved to be better than the remaining ones,  $\text{MnO}_2$  SCS. The tests in wet conditions, the tests for the study of stability, time on stream and cyclical, and the reproducibility tests are conducted only using  $\text{MnO}_2$  SCS. As regards the operating conditions, the stream entering the reactor has a pollutant concentration equal to 100 ppm, 21% vol of  $\text{O}_2$  and nitrogen to balance, reaching a total flow rate of 50 ml/min. The goal is to obtain complete conversions, for all three sample molecules, below  $300^\circ\text{C}$ , keeping us in low temperature conditions. Subsequently we try to understand how stable the best performing catalyst is over time both in the presence and absence of water. Finally, through reproducibility tests it will be possible to understand whether the results obtained can be repeated by different operators, at different times, guaranteeing the possibility of continuing the research.

## **1.2 Indoor air pollutants**

The indoor air quality has, today, a fundamental importance to prevent serious diseases onset. Already from before Christ the Greeks and Romans were aware of the detrimental effects that the polluted air of cities and mines could cause on the population. Dickens himself, through his books, accurately described to us the terrible conditions of those living at the end of the 1800s in the suburbs of London where soot dirtied the walls of the houses and drinking water was a luxury. In the 1781 Lavoisier, by studying the human metabolism, has been capable to conceive a way to measure the quality of the air based on the relative concentration of oxygen and carbon dioxide. And John Griscom, a New York surgeon, in the 1850 said “deficient ventilation ... (is) more fatal than all other causes put together”. (Sundell, 2004)

After this premise on indoor pollution, we can consider all those harmful compounds found within confined environments, and which affect indoor air quality (IAQ). Substances that can alter air quality are classified as physical, chemical, or biological agents. (Hannah Blair, 2023) This last category

includes not only biological contaminants such as mould, fungi and bacteria but also bio-effluents, i.e. those unpleasant-smelling chemical compounds produced by the human body. They do not reach concentrations that are hazardous for health, but they affect the general well-being of those present. Notoriously, an environment with poor air circulation and a high number of people is prone to having "stale" air. Furthermore, humans and animals tend to release biological contaminants due to peeling of the epidermis and hair loss. Furthermore, gestures such as sneezing, coughing and speaking produce tiny droplets of flugge and saliva which contribute to the increase in biological contaminants. So, air circulation systems play a crucial role in air quality indices, they must be designed and maintained in the best possible conditions, so as not to be the first source of pollution.

Secondly, combustion processes must be considered, these are closely related to the individual's activity: smoking, cooking, space heating. First of all passive tobacco smoke (ETS) followed by fossil fuels such as coal, oil, kerosene and stove gas and wood contribute to the increase of carcinogenic and toxic substances such as nitrogen oxide and dioxide (NO, NO<sub>2</sub>), carbon dioxide (CO<sub>2</sub>) and carbon monoxide (CO), soot, polycyclic aromatic hydrocarbons. The third source of indoor pollution includes building materials and home cleaning and body care products. In this case, the emissions persist throughout the entire life cycle of the building. The greatest risk is represented in the phase following the completion of the structure when the quantity of VOCs emitted is drastically more significant. (Europe, 1989) More in-depth analyses bring to light how emissions of substances are relatively high in the first period immediately after complete construction and which decrease after about six months until disappearing within a year. Subsequently, the phase of secondary emissions begins. This phenomenon is caused by the iterations of the surface with different thermal and chemical treatments (seasonal temperature changes, use of cleaning products, waxes or paints). Glues, adhesives, solvents, and hobby products such as plotters and photocopiers should also be included as sources of indoor pollution. (Principali inquinanti indoor e loro fonti, 2015)

The main air indoor pollutants are particulate matter (PM), nitrogen oxides (NO<sub>x</sub>), sulphur oxides (SO<sub>x</sub>), carbon monoxide (CO), volatile organic compounds (VOCs). (Paul B. Tchounwou, 2021)

To summarize, the sources of indoor pollution are mainly due to combustion phenomena, the use of certain chemical products and certain construction or furnishing materials. Finally, it is important to consider that these emitted molecules can react with each other and produce highly reactive compounds that are not so easy to measure but that can harm the skin or mucous membranes. (Sundell, 2004)

### **1.3 Consequences of indoor pollution**

It is noted that over the last thirty years the incidence of asthma and various types of allergies has increased, pushing the scientific community to believe that this phenomenon is not due to a genetic modification, but rather to an alteration of the surrounding environment. (Sundell, 2004)

The air pollution is the first cause of fatal illnesses such as acute respiratory illness, ischemic heart disease, cerebrovascular disease, and lung cancer. Up to date, the statistics report that 9 out of 10 people breathe air whose concentrations of certain substances is beyond threshold limit value (TLV). The TLV is a measure of the concentration limit that a single person can be exposed without damages. At the same time, it is difficult to precisely discern the responsibility of indoor environment in comparison with outdoors. Although indoor air pollution is considered the cause of diseases of greater importance than the sick building syndrome (SBS) such as respiratory infections (ARI) and multiple chemical sensitivity (MCS); the SBS can be considered the symbol of the extreme consequence of a lifestyle which today is very common in more developed countries such as Europe or the United States. The SBS (sick building syndrome) was introduced, for the first time, by the WHO (World Health Organization) in 1983 and from that moment the apprehension about this phenomenon increased year after year, until it exploded with the advent of the Covid-19 epidemic in 2020. Following the energy crisis of the 70s, to avoid excessive heat dispersion, the air recirculation processes in heating and ventilation systems were increased. This brought to attention the prevalence of peculiar symptoms in certain buildings such as respiratory system diseases or very strong allergies to dust. In these forty years, the countries that have most thoroughly studied the causes and consequences of this syndrome have been the United States and Denmark, followed by Sweden with reference to Uppsala University and the research immediately highlighted how SBS and air quality were intrinsically connected. A recent study demonstrates that it has become a serious health problem with an incidence of 23-41% in university administrative buildings. (Wang, 2022) The common symptoms SBS extend from a simple headache to several kinds of irritation and cause damages to health and productivity. The main four subjects in SBS research comprehend Toxicology, Allergy, Medicine General internal and Immunology. According to statistics, the subjects most affected by SBS are women, office workers and children as their stay in closed environments is greater. The causes that lead to the onset of this syndrome must be sought in insufficiency of thermal comfort, air conditioning pollution and finally air pollution. Thereby the risk factors consist of the presence of compounds such as volatile organic compounds, microbial factors (mold, fungi, bacteria), dust bioaerosols. The concomitance of all these factors therefore determines not only the worsening of diseases, for example asthma, allergies, chronic fatigue syndrome etc. in subjects already at risk, but

also the onset of them. (Bergefurt, Weijs-Perree, Appel-Meulenbroek, & Arentze, 2022) Not to mention the terrible consequences on mental health.

In conclusion, we can certainly assume that from 1970 to today the situation has certainly not improved, although we are more aware of the presence of toxic substances in our homes or working environments. The new building technologies, despite being designed for greater energy saving, are made up from materials that emit harmful substances. The use of certain paints or glues which are usually used for the manufacturing of low-quality furniture decreases the emission of toxic volatile substances over time, but on the other hand as they degrade, they produce new ones which the effects on human health are often ignored. Furthermore, although ventilation is an effective method for renewing the air in a short time, it cannot be considered a definitive solution. For these reasons, many companies today have focused on developing products that guarantee the reduction or adsorption of harmful volatile compounds.

#### **1.4 Italian regulations for VOC concentrations**

At Italian level, the UNI 10339 regulation of 1995 provides for the delineation of ventilation systems and the intended use of a specific building, through a prescriptive approach, i.e. estimating the minimum and maximum air flow rates per person, or per square meter of surface. To date, this legislation is subject to revision to align with the new directives of the European Union which refer to the document EN 13779 of 2007 sanctioned by the Technical Council CENT/TC 156 regarding the "ventilation of structures". Reference is made to the design of the air conditioning system of rooms in non-residential buildings. The document is composed of an initial classification of the air, and a list of possible internal air control systems (IDA-C). It moves on to a more accurate description of the internal environment and agreements on project criteria based on the general data of the buildings (such as position, external climate data, etc.), and the internal activities (residential use, catering, workshop, etc.). The air is classified, according to the area in which the structure is located, and is defined as exhausted (EHA), extracted (ETA), external (ODA) and internal (IDA) and supply air (SUP). According to the relative level of pollution the air is labelled with a number from 1 to 4. In this regard, in the evaluation of the air quality index, the presence of typical pollutants such as carbon and nitrogen monoxide and dioxide and the more harmful VOCs such as benzene, formaldehyde and polyaromatics must be considered in relation to their reactivity. (UNI EN ISO159, 2003)

Another relevant section is that relating to the humidity of the internal air in relation to the thermal comfort of the individual which stands at around 30% -70%. Given that the droplets of water vapor

suspended in the air and in contact with surfaces facilitate the proliferation of mites, fungi and other biological contaminants, it is in any case necessary to avoid an increase of humidity level.

The Ministry of Health with the Legislative Decree 27 March 2006 n.161 on: Limitation of emissions of VOCs due to the use of organic solvents in some paints and varnishes subordinates the market introduction of several building products such as paints or coatings. In the first part of the document, it is specified the potential sources in indoor environment of different VOCs. In particular, the decree focuses on several topics: the maximum content of VOC according to the category, analytical methods for calculating the rate of VOC, labelling obligations, finally the possible sanctions are outlined. (Xueyang Zhang, 2017-09-15)

The decree also establishes the precautionary measures that the single individual, in his little, can adopt. It is essential to choose materials that do not contain, or trying to limit as much as possible, VOCs, such as water-based paints, to adequately ventilate living and working spaces and to regularly check household appliances such as stoves or printers, finally equip closed environments with adequate filtering and ventilation systems.

## **2 State of the art**

A class of molecules which, today, has a crucial role in determining the severity of pollution in a indoor environment is VOCs (volatile organic compounds). At a scientific and legislative level, a VOC is defined as any substance which at a temperature of 298 Kelvin degrees and atmospheric pressure has a vapor pressure equal to or greater than 0.01 Kpa. (Paul B. Tchounwou, 2021) A large number of substances fall into this category of compounds: aliphatic, halogenated, aromatic hydrocarbons, alcohols, aldehydes together with their main sources ranging from fuels to detergents, diluents, pesticides. Nonetheless, toluene and formaldehyde are significant: the first due to its high diffusion in residential environments and the latter due to their toxicity and mutagenicity.

How can we reduce emissions instead?

Countless VOCs abatement technologies have been invented each with advantages and disadvantages: from photocatalysis to the use of ozone, the adsorption, membrane separation, biological degradation, thermal incineration. However, a trade-off must be found between performance and cost. Furthermore, it must be considered that this application must be inserted within domestic or working environments and therefore must have characteristics compatible with this type

of residential structures. This technique involves the use of specific catalysts which convert the molecules concerned at temperatures lower than those of normal decomposition. For this reason, catalytic oxidation is a good compromise in terms of energy expenditure, cost and efficiency. Today, scientific research has brought to light the possibility of exploiting new types of nanostructured catalysts based on transition metal oxides such as Cobalt, Iron or Manganese. Among the many techniques for the synthesis of oxide-based catalysts, one that is particularly efficient and competitive in terms of yield and time required is the Solution Combustion Synthesis (SCS).

Let's focus now on the topic of VOCs. The breathed daily air is composed of a variety of different compounds such as VOCs. As the name suggests, they are volatile at room temperature and at atmospheric pressure. The general definition of the Code of Federal Regulations reports: *“Volatile organic compounds (VOC) mean any compound of carbon, excluding carbon monoxide, carbon dioxide, carbonic acid, metallic carbides or carbonates and ammonium carbonate, which participates in atmospheric photochemical reactions, except those designated by EPA as having negligible photochemical reactivity”*. (EPA's Terms of Environment Glossary) The scientific literature uses a more accurate definition that is consistent with indoor VOCs: *“Volatile organic compounds, or VOCs are organic chemical compounds whose composition makes it possible for them to evaporate under normal indoor atmospheric conditions of temperature and pressure”*.

These compounds can be the result of specific chemical reactions take place every second in the air, and actively participate and be converted into simpler molecules, such as carbon dioxide and water vapour. As previously cited, they are present in both indoor and outdoor environment. They have become, during the last fifty years, indispensable ingredients in most products. They are ubiquitous in household and furnishing or building materials such as paint, solvents; in addition, people and the activities done in closed environments, like cooking, smoking and even cleaning, leads to the generation of high levels of VOCs. Furthermore, it is important to count the income deriving from outdoor traffic and industrial emissions. Indoor VOCs can potentially be extremely harmful on the long period to people that are exposed. The effects of VOCs could affect immune to cellular and cardiovascular to respiratory apparatus. Furthermore, they are considered as a cause of the climate variation as well as the formation of ground level aerosol, smog and ozone.

The World Health Organization categorizes indoor volatile compounds as:

- Very volatile organic compounds (VVOCs)
- Volatile organic compounds (VOCs)
- Semi-volatile organic compounds

The lower the boiling point is, the more easily the molecule is emitted from a specific surface or product. (Europe, 1989)

**Table 1** VOCs classification due to the boiling point range

Description	Abbreviation	Boiling Point Range	Example Compounds
Very volatile	<b>VVOC</b>	<0 -100	Propane, Ethylene, Propylene butane, methyl chloride
Volatile	<b>VOC</b>	100-240	Toluene, acetone, ethanol
Semi-volatile	<b>SVOC</b>	240 a 380	Phthalates, pesticides

So, it is evident that avoiding from entering in contact with them is impossible. The unique solution is the elimination of them through different techniques of abatement. There are five classes of VOC which allows them to be differentiated according to their chemical, electronic and physical-chemical properties. This is a class that includes more than 300 chemical compounds including aromatic, aliphatic, oxygenated, halogenated, N and S containing VOCs. For this reason, the problem of reducing VOCs is particularly complex. Numerous factors must be taken into consideration such as the acid-base properties of the support, the method of preparation of the catalyst, the operating conditions in order to define the best catalyst in terms of efficiency, activity, selectivity and resistance to poisoning.

Famous for their harmful effects on human health are benzene and formaldehyde and some polyaromatics. The former is part of the class of aromatic compounds together with toluene, ethyl benzene and xylene (BTEX) characterized by the presence of the benzene ring which makes them extremely resilient and require high temperatures to be converted. Formaldehyde is characterized by a pungent odour and is produced during the combustion process as tobacco smoke and emitted by substances such as resins composed of urea and formaldehyde (used for thermal insulation) and fabrics that have undergone anti-crease treatments. It is part of the OVOCs together with alcohols, ketones and ethers. Considering indoor environments, the concentrations of this substance are ten times higher than outdoor ones (from 10 to 50 microg/mc). The highest concentration peaks were recorded in prefabricated houses, and in buildings that have undergone recent construction interventions. (Yunlong Guo, Recent advances in VOC elimination by catalytic oxidation technology onto nanoparticles catalysts: a critical review, 2021)

Aliphatic compounds, on the other hand, are generally emitted from natural sources or from petroleum processing and are classified as alkanes, alkenes or alkynes depending on the degree of unsaturation of the molecule. In addition to having a harmful effect on the health of living

beings, they can lead to the formation of OVOCs and aerosols by reacting through photochemical processes. Within this work, two of the three molecules that are used as pollutants are ethylene and propylene. (Zhang, 2016)

## **2.1 VOC abatement techniques**

Considering the huge impact that these substances have, over the years various technologies have been formulated with the aim of recovering them, whether the VOC can be considered recoverable, or eliminating them permanently. So generally, there is a primary distinction between recovery methods and destruction methods. The first comprehends techniques such as adsorption, condensation, membrane separation. As we will see later, they are very common methodologies as they do not require too high an investment and the complexity of the system is not so complex. On the other hand, more radical solutions are incineration, photocatalytic oxidation, ozone oxidation, catalytic oxidation, plasma catalysis and biological degradation. They consist mainly in conversion of VOCs into H<sub>2</sub>O and CO<sub>2</sub>, and some of them require a vast amount of energy to reach the required temperature. Furthermore, the risk of produce toxic byproducts such as NO<sub>x</sub>, ozone or radicals is constantly present. (Z. Zhang, 2015)

Some solutions, as the recovery methods, adopted nowadays on a practical level do not provide for the effective conversion of VOCs into molecules that are less harmful to humans. Many texts report the use of specific materials for the adsorption of these substances; but, in the end, these techniques foresee only the removal of these molecules using efficient ventilation systems and not the elimination from the environment. At the same time, it is constant the risk of desorption of these molecules. Furthermore, it is relevant to underline the need of maintenance and the necessity of having to change the material after a certain period. So, in many cases even if the adsorption techniques are evidently more achievable and cheaper, they are not a definitive solution. (Hannah Blair, 2023)

To sum up each of these technologies has advantages and disadvantages, not to mention that the abatement efficiency is directly proportional to the cost of the technology used. (Europe, 1989)

We will now analyse the technologies individually, indicating their potential and the limitations encountered to date, focusing on oxidative catalysis. This technology is the right compromise between plant cost and process efficiency. It is essential to consider the specific situation we are dealing with indoor non-industrial environment; in this case the solutions must be compatible with a system where



the temperature has to be under specific values and the human safety and comfort are to be considered as the priority. There is no universal solution to the problem of indoor pollution and each technology has a wide range of specific applications. In each step of the research, multiple aspects must therefore be considered: operating conditions, available material, surrounding environment, molecules to be broken down and so on. Finally, after careful analysis, a compromise can be reached as with any other choice.

### **2.1.1 Adsorption**

One of the most famous and common VOCs removal technology is undeniably the adsorption, which exploits a wide range of materials from mesoporous to microporous. Generally, they are carbonaceous materials with a pore size distribution that enables to capture VOCs. The interaction between two different compounds can be characterized by a different nature such as hydrophobic effect, hydrogen bonds, Van der Waals interactions covalent and electrostatic interactions and  $\pi$ - $\pi$  bonds. In particular the carbonized adsorption phase attracts pollutants through electrostatic attraction, non-polar organic attraction and polar organic attraction. The key factors controlling the adsorption onto engineered carbon materials are the specific surface area, pore size, surface chemical functional groups, bulk density. (R. Nikam, 2017)

Whenever an adsorption phenomenon occurs, the specific surface area is analysed to comprehend the sites' availability for the process: the larger the better. To open paths in inaccessible pores or to create new crevices in the materials, the methods generally adopted are impregnation, heat, acid, or base treatment and eventually the use of microwave, ozone or plasma. Each of these must be accurately projected because the collapse of pores is always around the corner. As catalysts even for adsorbent material the highest surface area doesn't always correspond to an improvement in the performance. Based on the size of the pore, they can be divided in micropore ( $D_p < 2\text{nm}$ ), mesopore ( $2\text{nm} < D_p < 50\text{nm}$ ) and macropore ( $D_p > 50\text{nm}$ ). The third cited characteristic is the presence of surface chemical functional groups beside the morphology structure. Beyond a simple synthesis technique several activation or modification strategies contribute to enrich the surface of compounds that increase the physical or chemical interaction of the two interested phases, in order to increase the bond specificity. Then the bulk density represents the capacity of carbonaceous material to englobe a major quantity of VOCs. (Paul B. Tchounwou, 2021)

At the same time, it is compulsory to consider not only the adsorbent but also the adsorbate material and its peculiarities such as polarity, molecular, structure, boiling point etc. In general, this argument applies not only to adsorption but to all subsequent technologies.

It has been demonstrated that, when the pore size is equal to the adsorbate size, optimal adsorption occurs. Examples of these are activated carbon fiber (ACFs), carbon nanotubes (CNTs), graphene, carbon-silica composites (CSCs), carbon cryogels microspheres (CCMs) etc.. (Xueyang Zhang, 2017-09-15)

In conclusion, these materials have excellent adsorption capabilities, and the modification of their structure is not extremely complex. Their cost is extremely low although research is working to further reduce it. (Haibao Huang Y. X., 2015) Despite all this, they are to be considered only as a recovery technique and not for culling. Secondly, as the boiling point increases, the complexity of the chemical structure of the VOC and the possible presence of humidity affect the adsorption efficiency.

### **2.1.2 Photocatalytic oxidation (PCO)**

The use of photoexcited photocatalyst is nowadays one of the most advanced technologies in the field of air pollution abatement. Its peculiarities are considered extremely unique: the direct use of solar light, the possibility of exploit the air pollutants as fuels. For example, the carbon monoxide could possibly be converted in methane and carbon monoxide. Moreover, the process is self-cleaning and potentially it can be utilized both indoors and outdoors under LED lights or solar rays.

Eventually it is suitable not only for inorganic pollutants such as NO<sub>x</sub> and VOCs but also for biological menaces such as fungi, bacteria and mould. (Zeesham Ajmal, 2022)

The keys to reach its success are the reactor design and the features of the photocatalytic material. It is easy to conceive the importance of the catalyst in order to have a required specificity and to prevent from deactivation due to the deposit of waste such as soot or dust. Finally, a serious limit is the presence of water vapor. To date, the risk of inactivation and the models that allow us to understand the phenomenon of adsorption of molecules on the surfaces of these materials are still an open challenge for the scientific community. Despite this, the use of conjugated polymers (CPs) gives us hope for future developments. Their behaviour appears to be like some inorganic semiconductor oxides, providing characteristics that the latter do not possess, such as a larger visible light response and a better morphology and porosity.

However, as the other more recent technologies, the related issues are more relevant than the advantages of their use in the real practice. On a theoretical level there are a number of systems that can be exploited but the transfer to reality is still far away not only at a technological level but also at a cost level. (Zeesham Ajmal, 2022)

### **2.1.3 Plasma catalysis for VOCs oxidation**

The combination of the catalysis with non-thermal plasma guarantees unique advantages in the abatement VOCs field. But firstly, we have to make a briefly description of what effectively the non-thermal plasma is.

This specific material state is composed of electrons that have been accelerated by an electric field reaching a temperature up to 250.000°C. The system results to be, as a consequence, thermically unbalanced, the electrons of the plasma this excitation state to the gas molecules which emit photon or heat, producing ions and radicals. The process is extremely reactive, and it could be led to a number of different byproduct. For such reason the presence of the catalyst is meant to encourage just certain reactions.

This process is strongly recommended for hazardous VOCs such as chlorinated, fluorinated, brominated compounds and formaldehyde. The presence of plasma lead to the creation of chlorine radicals which can provoke chain reactions. (Satu Ojala, 2011)

In any case, as with photocatalysis, plasma catalysis is still a newborn technology that is technically feasible but applications in the practical field are struggling to arrive. In addition to the application limit, the economic aspect must also be considered as plasma is extremely expensive. (Hyun-Ha Kim, 2021)

### **2.1.4 Incineration or thermal combustion**

As the names suggest these techniques take advantages of high temperature to decompose bigger and more complex molecules in smaller ones by raising the operative temperature above thei autoignition point in presence of oxygen. The incineration can be performed with or without using a catalyst and it is a common methodology exploited at industrial level to purify air stream from VOC, particulate matter (PM) to send into the atmosphere. Depending on the design criteria the destruction efficiency ranges from 98 to 99,9% and for certain halogenated VOCs the required temperature is among 1100 °C. It is a technology quite mature: the first incinerator has been projected in 1940 and in comparison, with one without catalyst is less energyvory. Furthermore, the presence of a catalyst prevents from the formation of NO<sub>x</sub>.

Although the efficiencies are very close to 100%, it is a technology that can only be exploited on an industrial level as the presence of pollutants in the gaseous stream must be greater than 20%. They are mainly used for the abatement of mixtures containing halogenated or sulfur-containing compounds. Finally, they are particularly expensive due to the operating conditions that require a high use of fuel. (EPA-452/F-03-022)

### 2.1.5 Catalysis for VOCs abatement

One of the most captivating fields of chemistry is catalysis, as a matter of fact the 85 % - 90% of industrial processes include at least one catalytic step. Especially, nowadays, in the environmental chemistry the catalysis is exploited in oxidation, photocatalysis, biomass conversion. (Haibao Huang Y. X., 2015)

Exploiting a catalyst is the key to an infinite series of chemical reactions that otherwise would not be kinetically possible. The term “catalyst” is used to define any kind of compound or molecule that increases the rate of a reaction without taking part in it, in fact they simply lower the level of activation energy. The contact of the reactant with the catalyst’s surface, and the consequent establishing of a bond, makes possible the process of conversion into the desired product. Consequently, the product’s bond with the catalyst is broken and the formed molecules get away.

So, the process can be summarized in three main steps:

- Formation of bond of catalyst and reactant
- Occurring reaction
- Realising of the product

If the phase of the catalyst is different from that one of the reactants, the catalysis is labelled as heterogeneous, typically the catalyst is in the solid phase. It is essential in this specific case, where there are a gas and a solid, the diffusion of the gas from the bulk to the interface gas-solid and consequently in the internal porosity of the catalyst until reaching an active site. In fact only on this site it is possible that the reaction occurs. So, the adsorption of the reactant happens and the conversion. Finally, the product is desorbed and through a diffusive motion the molecules move away from the active site to return in the bulk of the fluid. During the experimental procedure it is essential to identify which, of these steps, is the slowest or the controlling step. It is precisely this step to affect the global reaction rate. (Fogler, 1999) The three most crucial peculiarities of a catalyst are the activity, durability and selectivity.

The abatement of VOCs can be performed in an efficient, environmentally safe, and cheap way using certain kinds of catalysts, even if, because of the immense variety of VOCs, the process is more complex, and it doesn’t exist a straightforward solution. (Satu Ojala, 2011) It is first necessary to distinguish, according to the environment in which we find ourselves: indoor or outdoor. In this case, the focus is environments for human use whose temperatures, for reasons of comfort and health, must not exceed certain thresholds. Furthermore, oxidative catalysis at low temperatures is advantageous as it avoids damaging the structure of the catalyst in the long term through sintering phenomena due to exposure to high temperatures. Recently, multiple efforts have been made to develop materials to

reduce the temperature of catalytic oxidation of VOCs. In general, two types of catalysts have been developed during the research for total VOC oxidation at low temperature: supported noble metals and transition metal oxides, but some research also reports the use of fibres, zeolites and mixed metal oxides. (Teresa Gelles, 2020)

So, we are talking about mild/low temperature catalyst.

Catalysts based on noble metals and metal oxides can destroy VOCs at temperatures that normally do not exceed 400°C. The use of noble metals such as Pt, Ru, Au, Ag and so on allows the operating temperature to be further lowered by approximately 200°C in some cases it is possible to convert even at ambient temperature. They are famous precisely for their high activity at low temperatures; they are often used in the treatment of exhaust gases from machines and in selective reduction catalytic reactions. Generally, these metals are found dispersed on a porous support characterized by a high mobility of the oxygens of the crystalline lattice. For this type of application the materials used are aluminosilicates, perovskites or simply metal oxides. In particular, when it comes to low-temperature oxidative catalysis, the synthesis method and the active sites present on the surface of the catalyst play a fundamental role.

We know, however, that these materials are extremely sensitive to the presence of poisons such as water, coke, and chlorinated oxide with sometimes irreversible effects. Furthermore, they represent a limited natural resource. The fragility and the scarcity of these materials is therefore a potential economic and technological damage that cannot be ignored. Consequently, the use of less valuable but more resistant materials such as transition metal oxides is often preferred. For many years now they have been exploited not only as a support but as actual catalysts for oxidation reactions. (Zhang, 2016)

In conclusion, before delving into the metal oxide sector, let's remember why oxidative thermal catalysis at low temperature is one of the most developed and applied technologies to date. Firstly, for the high level of safety, for the low cost of the designed system and the catalyst and finally for the environmental friendliness. (Haibao Huang Y. X., 2015)

To evaluate the performance of the catalyst, the conversion ( $X_{Vocs}$ , %) in relation to the temperature is generally taken into consideration to obtain 10%, 50% and 90% conversion ( $T_{10\%}$ ,  $T_{50\%}$ ,  $T_{90\%}$ ). All this provided that the same operating conditions are maintained.

### **2.1.6 Transition metal oxides catalyst**

As previously mentioned, due to the scarcity of noble metals and their rather high cost, transition metals were taken into consideration in order to achieve similar conversion rates at the expense of

an increase in operating temperatures. In the periodic table the metals are shown in groups III B and II B

Below are some of the most important characteristics that are analyzed to understand the catalytic role of the transition metal in oxidative reactions at low temperatures:

- Metal-oxygen bond
- Host structure
- Redox properties
- Lattice oxygen
- Multifunctionality of active sites

Most industrial catalytic processes involve metal oxide catalysts such as silica, zeolites, titania. They are considered a class of inorganic compounds with various peculiarities and applications. In particular, scientific research has made enormous efforts in the attempt to create materials based on metal oxides that are economical and with a good level of performance. The structure of the oxide can be porous, mesoporous, or complex and this led to specific properties such as acidity, basicity, redox features. Particularly, the acidity of the species on the lattice is important for the oxide, because of its correlation with activity. At an application level, p-type metals are favored over n-type ones. The difference between the two lies in the atomic structure: the p-type ones have an adsorbed  $O^-$  while the n-type ones have an adsorbed  $O^-$ . the adsorbed oxygens are more mobile and reactive than those that are directly part of the lattice, i.e. the reticular oxide ions  $O^{2-}$ . (Prasad, 2019) Furthermore, the surface presents a series of defects as well as terraces, kinks, steps which causes a relevant role in the catalytic activity. (Vedrine, 2019)

Group II-B and III-B metals are notoriously known for their multivalent atomic configuration which allows them to form numerous configurations. (Zhang, 2016) In fact, by exploiting common and easily extracted metals, such as iron or manganese, and simple and relatively fast synthesis techniques such as SCS, it is possible to obtain a highly competitive product on the market whose features are corresponding to those of an indoor material. (Yunlong Guo, Recent advances in VOC elimination by catalytic oxidation technology onto nanoparticles catalysts: a critical review, 2021)

### 2.1.7 Manganese oxides catalysts

In comparison with other transition metals manganese result to be more active at lower temperature and thermally stable, so it is exploited for the oxidation of many VOCs. Many articles report the effective use of this compound for the oxidation of ethanol, toluene, and ethyl acetate. It has been extensively studied for its low toxicity, durability, and activity. This is related to the possibility of manganese of manganese to form different oxides with different oxidation number:  $Mn^{2+}$ ,  $Mn^{3+}$ ,  $Mn^{4+}$ . The possibility of change the oxidation state and having structural defects permit to the oxygens to improve their mobility on the surface of the material. This element has an enormous range of crystal phases ( $\beta MnO_2$ ,  $\gamma MnO_2$ ,  $\alpha Mn_2O_3$ ,  $\gamma Mn_2O_3$ ,  $\alpha Mn_3O_4$ , and  $MnO$ ) and it is possible to obtain different form of catalysts 1D tunnel structures, 2D layer phases, and 3D spinels. (Alain Manceau, 1992)

Manganese oxides such as  $Mn_3O_4$ ,  $Mn_2O_3$  and  $MnO_2$  are famous for their high activity in the oxidation of hydrocarbons. From economic point of view, they are considered cheaper than others and environmentally friendly materials. Consequently, it had been attempted to use them as catalyst due to their extremely relevant efficiency in the oxidation cycles. As a single component, a precious metal catalyst is absolutely the best in comparison with a base metal oxide; but due to the limited availability and the higher cost of noble metals an attempt was made to combine the two. The capabilities of the latter are deeply enhanced by the combination with other elements such as gold, platinum. In nature there are three original types of manganese oxide with square tunnel size: pyrolusite, cryptomelan and todorokite. In order to guarantee the best possible performance, it is necessary to consider the effective tunnel diameter of the manganese oxide in comparison with the dynamic diameter of the molecule considered. (Haibao Huang Y. X., 2015)

The main solid from which manganese is extracted is pyrolusite. Within this discussion, particular attention is paid to manganese dioxide. It appears as a black, odorless powder. The main use of manganese dioxide is in the battery sector and as an oxidizer in organic reactions. Its activity depends intimately on the synthesis method through various complex techniques it is possible to obtain particularly active and resistant nanostructured materials.

Manganese dioxide, through previous studies conducted by Piumetti et al. it was found to be the best of the various possible oxides that manganese can become. (Sang Chai Kima, 2010) For this reason the study focuses on  $MnO_2$  SCS. It is a polymorphic material, this means that for the same oxide there are several phases:  $\alpha$ ,  $\beta$ ,  $\gamma$ .

### **2.1.8 Theoretical basis for the synthesis**

The main purpose of a synthesis method is not just to produce the desired material but also to obtain certain qualities such as a specific surface area and a uniform distribution of the pores, furthermore in some cases it is need an adequate mechanical resistance and yeald strength.

The literature divides the methods of synthesis in two big categories: via precipitation or combustion synthesis. The first one consists in the generation of the solid phase through a decomposition or precipitation reaction. The active phase, in this case, is fixed on a solid already present. During the process the obtained powder will be deposited on the support.

The second instead includes the SHS (self-propagating high temperature synthesis) developed in 1967 by Mezhanov, Shkiro e Borovinskaya. It consists of an exothermic reaction who result to be extremely rapid and self-sufficient: the heat released by the reaction is equal to maintain the reaction itself, however it is required to reach the autoignition temperature to boot the process.

An alternative method to SHS is represented by SCS (solution combustion synthesis) proposed by Patil and Kingsley. In this work this technique is exploited to obtain a mesostructured oxide. (Alexander S. Mukasyan, 2007)

### **2.1.9 Solution Combustion Synthesis**

Around the 1980s, a turning point that allowed the discovery of this new synthesis method was the low-temperature decomposition (150-250°C) of hydrazylcarboxylate hydrate. The complex structure of this nitrate salt allowed the fuel (represented by the H and C atoms) and the oxidant (i.e. the O atoms) to be present within the same molecule. The sum of the various reaction steps which are both endothermic and exothermic lead to obtaining a self-sustained reaction and to the production of a significant quantity of gaseous moles. The turning point, which led to a real SCS, was the use of a solution of distilled water based on aluminium nitrate hydrate as oxidizer mixed with urea as fuel and brought to a temperature of 500°C.

Precisely since SCS is a self-sustaining thermal process where the energy source is represented by the exothermic reaction itself, it becomes part of a broader category of synthesis techniques conventionally defined as SHS or self-propagating high-temperature synthesis or more simply combustion synthesis (SC). But it must still be recognized that this technique has unique characteristics compared to classic SHS and it is precisely these peculiarities that make the final product perfect for catalytic oxidative reactions at low temperatures. First, this technique is specifically used to synthesize materials such as metal oxides or metals. Secondly, the procedure



begins by preparing an aqueous solution where there is the metallic salt, in this case a nitrate, and the fuel (generally an organic molecule such as urea or glycine). This step allows the reagents to be dispersed at a molecular level within an aqueous solution allowing to obtain as a result a product with a uniform formulation on a nanometric scale. Finally, as previously mentioned, the final result of the reaction is the production of a significant quantity of gas which involves an expansion and a rapid lowering of the temperature of the mixture. These two phenomena allow us to obtain a porous and highly dispersed solid. (Arvind Varma, 2016)

The reagent mixture requires three components which are defined as oxidizer, fuel, and solvent. Generally, the oxidizer can be a metal nitrate, a nitrate hydrate, ammonium nitrate or nitric acid. The fuel instead can be urea, glycine, or a sugar such as glucose or sucrose. Finally, water or alcohol, benzene or kerosene can be used as a solvent. Although the possible combinations may be varied, the main aim is to have a fuel and a solvent that are highly soluble in each other and that the nitrate is compatible with the fuel, without the risk of incurring an explosion. Furthermore, the fuel must have a decomposition temperature preferably lower than 400°C.

The SCS can be conducted according to two different protocols: volume combustion or self-propagating combustion mode. The first involves uniform preheating to the boiling point of the solvent. The second instead consists in the local heating of a small quantity of solution (1 mm) inside the reagent system. In the field of heterogeneous catalysis, the SCS technique is exploited to obtain bulk and supported catalysts. Among the numerous methods adopted to synthesize catalysts, the solution combustion synthesis (SCS) is certainly one of the most advantageous to obtain nano-structured materials.

Nowadays this technique is exploited in different application fields like heterogeneous catalysis, production of advanced materials for energy technology, thin films and nano-ceramics, biotechnology. Despite the simplicity of the synthesis method, the SCS method allows the obtaining of oxide powders with a high purity and with nanometric crystals. Furthermore, it is a technique that allows you to skip the calcination step usually required in classic sol-gel techniques.

The synthesis consists of three different steps: mixture preparation, reaction and cooling down. It all begins thanks to the decomposition and dehydration of the salt present in solution.

The procedure consists in mixing an aqueous solution of the metal precursor (manganese nitrate) and urea used as fuel. When the system reached the complete dissolution, the crucible was transferred in a oven where the reaction occurred at 400°C for 15 min. (Alexander S. Mukasyan, 2007)

The nitrates are specifically used because of the oxidizing nature of the NO<sub>3</sub><sup>-</sup> and due to the high solubility in water to have a sufficiently high concentration.

In conclusion, SCS is a simple technique that allows you to obtain nanostructured oxides with a high level of purity and crystallinity by exploiting a single self-propagated reaction which also acts as a calcination step.

In these specific experiments has been used the urea because it is more convenient for this particular case of study. (A.Kopp Alves et al, 2013)

### 3 Catalyst characterization methods

The following paragraphs indicate and describe the theoretical bases on which the characterization methods used during the experimental phase are based to describe the samples obtained from a morphological, structural and chemical point of view. Physisorption at  $-196^{\circ}\text{C}$ ,  $\text{H}_2$ -TPR temperature programmed reduction,  $\text{O}_2$ -TPD temperature programmed desorption, X-ray diffraction (XRD) and X-ray photoelectron spectroscopy (XPS), field-emission scanning electron microscopy (FESEM) were exploited. The simplifying hypotheses that allow the use of these methods and the equations on which they are based are cited.

#### 3.1 Nitrogen physisorption at $-196^{\circ}\text{C}$

The phenomenon of adsorption involves the enrichment at the interphase of one or more chemical species between two distinct phases. In this case it is a physisorption, which turns out to be not very specific: the interaction forces are dispersive, short-range repulsive and Van Der Waals forces. The gas adsorbs, forming a multilayer structure as the relative pressure increases. Depending on the probe gas used, various types of physisorption are defined. The process is conducted at constant temperature.

The Nitrogen physisorption method is used to calculate the specific surface area, the pore size distribution and the pore volume. These characteristics are strictly correlated to the quality and the behaviour of porous materials. This technique involves a pre-treatment phase in which the material inside a glass ampoule is heated to a temperature of  $200^{\circ}\text{C}$  for two hours to remove impurities present on the surface. After the burettes have cooled, the actual physisorption phase takes place: the burettes covered with a protective jacket are inserted inside the specific machine where the powder encounters nitrogen. The more time passes, the more layers of nitrogen adsorb on the surface, reaching a saturation layer, this first phase follows the adsorption curve. When the pressure ratio reaches unity the desorption phase begins. The two curves do not follow the same pattern, therefore a hysteresis phenomenon occurs. Therefore, from literature data we can determine the shape of the pores. (K. S. W. SING (UK & al., 1982)

and it follows the theory of Brunauer Emmett and Teller hence the name. It consists in the low temperature physisorption of nitrogen.

To calculate the SSA the theory is composed by a group of assumptions that must be confirmed. They are:

- The energy of adsorption of each layer is equal to the energy necessary to liquefy the gas, in other terms the rate of condensations is equal to the rate of evaporation.
- To describe the kinetic, of adsorbed layers it is possible to use the model of Langmuir.
- The forces of physisorption and the forces of condensation are similar.

It is essential to transform the isotherm of adsorption into the BET plot, in order to estimate the surface area. In a steady state condition, each layer can be described by the following equation:

$$a_i * p * \theta_{i-1} = b_i * \theta_i * \exp\left(-\frac{E_i}{RT}\right) \quad \text{Equation 1}$$

Where symbols represent

$a_i$  and  $b_i$  are adsorption and desorption constants.

$\theta_i$  fraction of surface covered by  $i$  layer

$p$ : Equilibrium pressure (Pa)

$E$ : energy of adsorption of the  $i$  layer (joule)

$R$ : ideal gas constant (joule/mol K)

$T$ : Temperature (K)

It is assumed that from the second layer the energy of adsorption is constant, thus the liquefaction energy ( $E_L$ ). Furthermore, if it is assumed a layer of infinite thickness when the pressure ( $p$ ) is equal to the saturation pressure ( $p^0$ ), the BET equation could be written:

$$\frac{\left(\frac{p}{p^0}\right)}{\left[n\left(\frac{1-p}{p^0}\right)\right]} = \left(\frac{1}{n_m C}\right) + \left[\frac{(C-1)}{n_m C}\right] \left(\frac{p}{p^0}\right) \quad \text{equation 2}$$

Where the symbols represent:

$n$ : Amount of gas adsorbed by unit mass of adsorbent.

$n_m$ : Monolayer capacity

$C$ : Empirical constant

The latter constant is related to the adsorption energy according to the following equation:

$$C = \exp\left[\frac{(E_1 - E_L)}{RT}\right] \quad \text{equation 3}$$

$$a_{BET} = n_m * L * \sigma \quad \text{equation 4}$$

Where:

$a_{\text{BET}}$ : Specific surface area

L: Avogadro constant

$\sigma$ : Area occupied by the adsorbate molecule

The BJH (Barrett, Joyner, Halenda) method is the most widely used in order to study the porosity. In this method the shape of the pores are cylindrical and are filled upon the condensation of the adsorbate. In the experimental phase the pores, by a reduction of the relative pressure, are emptied. The pore size distribution is expressed as the pore volume variation in function of the pore radius. To explain this behaviour is used the Kelvin's equation:

$$r_k = -\frac{2\gamma v_l}{RT} \ln\left(\frac{p}{p^0}\right)$$

equation 5

Where:

$r_k$ : Kelvin radius

$v_l$ : Molar volume of the condensate

$\gamma$ : Surface tension of the liquid condensate

R: ideal gas constant

T: temperature (K)

$P_0$  ambient pressure (MPa)

p :operative pressure (MPa)



**Figure 3.1** Physisorber of Nitrogen for physisorption Micromeritics TriStar II

### 3.2 X-Ray diffraction (XRD)

The objective of this technique is to measure the average spacing between the layers of atoms, determine the orientation of a single crystal or grain, or determine the crystal structure of a random

material and finally to analyse mechanic features connected to the material. In this particular case, it is used to verify if the synthesized solid is effectively the expected phase or if it is rather something else. This analysis is based on the Bragg's law expressed by the following formula:

$$2d \sin \theta = n\lambda$$

equation 6

Where the symbols represent:

d: space between atomic planes

$\theta$ : angle of coincidence

n: positive

The orientation of the plane is indicated by a set of coordinates which on the other hand represent each plane in the crystalline structure. Making then use of cell parameter, position of the given peak and a d-spacing formulas, which corresponds to each structure, we are capable to determine the relation between the related plane and the miller indices.

Therefore it is possible to understand, from a qualitative point of view, the phase of the sample. For our case, especially, it is known the atomic composition, so the phases can be determined by a comparison of the sample's peak intensities and their positions with some compounds of reference within a commercial database.

Second available information is the crystallite size; to determine such variable, it is used the Scherrer formula as follows:

$$\langle L \rangle = \frac{k\lambda}{\Gamma \cos \theta_0}$$

equation 7

Where the symbols represent:

$\langle L \rangle$  Average Crystallite size

k. constant dependent of the crystallite's shape

$\lambda$ : X-ray wavelength

$\Gamma$  : Diffraction width

$\theta_0$ : Bragg angle

It is assumed that the peak's shape is deeply influenced by size effects, and it correlates its size with diffraction width. At the end of the analysis through the software High Score Plus® it is possible to esteem the size by comparing the FWHM of our sample with the one of the lanthanum hexaboride from  $2\theta$  to  $0$  to  $40^\circ$  and making an average.

### 3.3 X-ray Photoelectron Spectroscopy (XPS)

It is part of surface analysis techniques such as Raman-IR and Auger. The X-ray photoelectron spectroscopy permits to obtain a series of information regarding the chemical surface composition, the overall electronic structure, and the chemical state. This elemental analysis is based on the photoelectric effect. This phenomenon has been discovered by Heinrich Hertz in 1887 who noticed that a surface irradiated with light was capable to emit electrons. It consists of the use of photons in order to remove the electrons from the material surface the samples are irradiated with x-ray not too strong (the energy is lower than 6keV). When a photoelectron is emitted, it means that a complete transfer of x-ray energy to a core level electron occurred. This can be translated in mathematical language as the following equation:

$$h\nu = E_k + E_B + \phi \quad \text{Equazione 8}$$

where the symbols represent:

$h\nu$ : photon energy

$E_k$ : kinetic energy

$E_B$ : binding energy

$\phi$  work-function term referring to the specific surface of the material.

In order to estimate the binding energy of an electron the equation is rearranged to obtain the  $E_B$

$$E_B = h\nu - E_k - \phi$$

It requires a minimal level of energy which corresponds to Work Material Function ( $\phi$ ). In this case we are analysing a metal, so the function  $\phi$  changes due to the crystallographic plane. By a measurement of the kinetic energy and the number of electrons that has been ejected, it is possible to deduce the chemical states, exploiting the principle of conservation of energy. (Siegbahn & Edvarson)The following equation is known as conservation of energy equation and more specifically as the photoelectric effect equation:

Primarily, such technique requires an extreme value of vacuum in the order of  $10^{-9}, 10^{-10} \text{mbar}$ . Then the surface sample is bombed by X-rays, the X-ray photon starts to interact with the shell electron exchanging its energy. This causes the generation of a photon that leaves the atom trading a certain quantity of measurably kinetic energy. The peaks are specific of the material, independent from the source of x-ray and are notated by the element and the orbital from which they have been ejected.

As the atomic numbers increases so a major number of electrons are attached to the nucleus and the higher is the binding energy. At the end the obtained graphic provides information on the signal intensity in comparison with the binding energy, the peaks positions enable to determine the chemical

composition and the element concentration is directly correlated to the intensity. Unfact each element produces a set of characteristic peaks due to the electron configuration within the atoms. (Ray, 2011)

### **3.4 FESEM**

The field emission scanning electron microscopy is a particular kind of microscope used to study the solid's morphology due to its capacity of providing high resolution images in comparison with the SEM (scanning electron microscopy). It can potentially furnish information on topography and elements. (Baldi, s.d.)

The technique on which is based this instrument is the following. An electron beam is sent to the surface of the sample by a field-emission cathode in the electron gun. Once that the electron reaches the sample, it starts to interact with it. There is a wide range of possibilities: it could be an emission of light, rejection of electrons back from the surface or emission of X-rays. The latter consequence may well be positive because usable to perform an elemental analysis the EDS (energy dispersive X-ray spectrometry).

Secondly, this fundamental interaction leads to the emission of secondary electrons, who could possibly be detected and used to create images. These images are useful to understand the morphology: the surface structure in general and as well analyse the shape and size of the pores.

It is crucial, in order to improve the quality of the images, making the surface conductivity as high as possible. If the sample has not this peculiar feature, it is likely to apply a metal coating, this can be modelled the thinnest possible through different methods.

### **3.5 H<sub>2</sub>-TPR and O<sub>2</sub>-TPD**

The temperature programmed reduction is a thermo-analytical technique focused to comprehend the reducibility of a sample. During the procedure the latter is put in a tubular reactor in order to be reduced by a gas flow (generally a mixture of nitrogen and hydrogen or hydrogen and argon) with an linear increase of temperature. A TDC (thermal conductivity detector) is placed at the end of the tube with the purpose of determining the outlet gas composition.

The reducible fraction of the sample reacts with the hydrogen of the reducing gas flow while the temperature increases. So as the temperature is rising the number of reducible species's moles tends to be zero until the end of the analysis. The maximum in the reaction rate corresponds to the maximum temperature. The procedure for conducting this characterization technique which aims to analyze the reducibility of the sample is now described. In a U-shaped quartz reactor, the catalyst powder is inserted between two layers of glass wool to avoid entrainment by the hydrogen and nitrogen stream. To avoid the instrument cut-off, the quantity of sample used is always less than 50 mg, as the intensity



of the peak is directly proportional to the mass. Before the test phase, the pre-treatment phase is conducted with a helium flow of 40 ml/min for a period of one hour and at a temperature of 400°C. At the end of the cooling, when the probe registers a temperature of around 50°C, the actual test phase can begin. The analysis involves a flow of 5% hydrogen in nitrogen of 20-25 ml/min. Hydrogen is the reducing gas while the inert gas is nitrogen. The system was brought up to a temperature of 700°C with a temperature increase of 5°C per minute. There are two temperature controls in the system, one in direct contact with the sample, the second inside the oven, as the exothermic reaction progresses the delta between these two temperatures becomes increasingly significant up to even reaching 10°C. The objective is to obtain a hydrogen consumption defined as (mmol/g<sub>cat</sub>). Through a thermal conductivity detector (TCD) it is possible to trace the presence of reduction reactions. In fact, it is possible to plot the signal as a function of the bed temperature and find the peaks related to a specific hydrogen consumption. The peak temperature is characteristic of the material and is linked to the reactivity of the species present on the surface of the catalytic powder.

## 4 Set up of tests

### 4.1 Dry tests with step

### 4.2 Catalytic Tests

The catalytic degradation performance of different molecules is conducted in a tube reactor of quartz (i.d. 5.0 mm) at atmospheric pressure within an electrical furnace to provide the heat in order to reach the required temperature for the reaction. The powder dosage introduced in the reactor is 50 mg on a bed of fiberglass, preventing the catalyst loss due to the speed of gas. The total feed gas current is maintained at 50 ml/min-1 and the concentration of O<sub>2</sub> is 21 vol% by mass flow controllers. This composition has been decided to recreate an ideal gas that can potentially be present in an indoor environment, according to the law of UE. Before each test, a one-hour pretreatment was carried out at a temperature 160°C with cylinder nitrogen to allow the desorption of any contaminants occupying the active sites. During this period the data were still recorded to monitor the temperature trend

### 4.3 Dry tests with steps

Below is a schematic figure of the system used to test the catalyst powder, obtained from the previous synthesis. The conditions we recreated mimic an indoor environment polluted with only one molecule at a time, in order to understand the progress of the conversion over time. There were available analysers exclusively for carbon monoxide and carbon dioxide. Therefore, not being able to have direct measurements of the concentration of propylene or ethylene, it was assumed that in the initial mixture the concentration of Co<sub>2</sub> was equal to that room temperature and that any increase, deriving from an increase in temperature, was directly correlated to a reaction occurred.

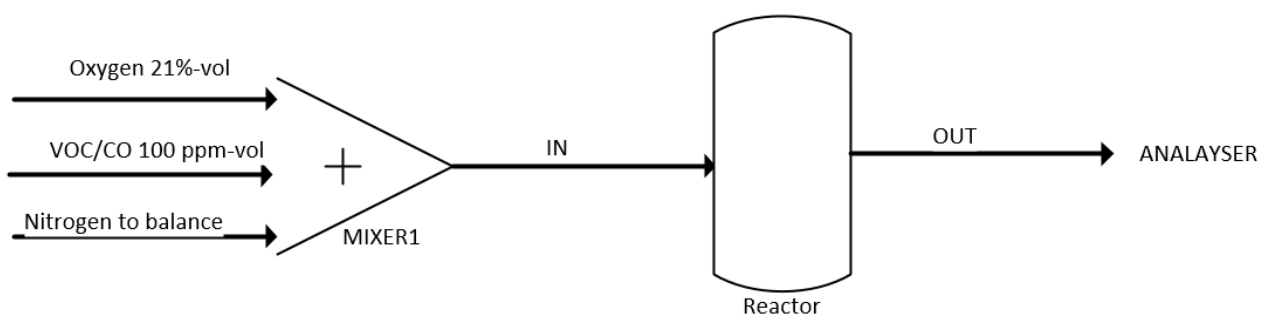


**Figure 4.1** Schematic figure of the experimental system

#### 4.4 Wet tests with steps

Now we move on to the test phase in which there is a certain concentration of water inside the reagent mixture. Since it is a more challenging operating condition, it was decided to use a single catalyst. The one that had previously proven to be the best, namely MnO<sub>2</sub> SCS. For this reason, in this experimental phase, the conversion capacity of the MnO<sub>2</sub> SCS catalyst has been analysed in conditions of relative humidity of 10% RH. The presence of water does not damage the structure of the catalyst, which is why it cannot be considered a poison. It is only a physical obstacle to the adsorption of pollutant molecules. Being a polar molecule, ethylene and propylene molecules, which are non-polar, are repelled by the surface of the catalyst and will need higher temperatures to be converted, a drexel was used to humidify the air. Using the following equation we estimated the RH, knowing the geometric characteristics of our device:

$$H = \frac{\dot{Q}_{liq}}{Av_g} \quad \text{equation 9}$$

Dove the reported symbols represent:

Vg Velocity of the inlet gas

A section area

H height of the tube immersed in hot deionized water

Subsequently, it was possible to obtain the relative humidity value.

$$\mathcal{L} = \frac{\dot{Q}_{gas}}{\dot{Q}_{Liq}} \quad \text{equation 10}$$

Dove the reported symbols represent:

$\dot{Q}_{Liq}$  the flow rate of liquid carried by the gaseous current.

$\dot{Q}_{gas}$  the incoming gaseous stream composed only of air.

$\mathcal{L}$ : humidity of the resulting stream.

Subsequently, the variations in performance in the presence of 10% RH are analyzed for the different molecules considered.

Below is a schematic figure of the system used to humidify and test the mixture. In particular, the drexel was positioned together with a coil inside a beaker on a heating platform such as to maintain the temperature inside the drexel at approximately 65 °C. The beaker contained deionized water to avoid the formation of limescale. Through a small tube connected to the oxygen and nitrogen mass flows, the air was bubbled inside the drexel. In this way a certain quantity of water was dragged along

with the current. The coil instead contained the mixture of air and oxygen in such a way as to be at the same temperature at the time of mixing.

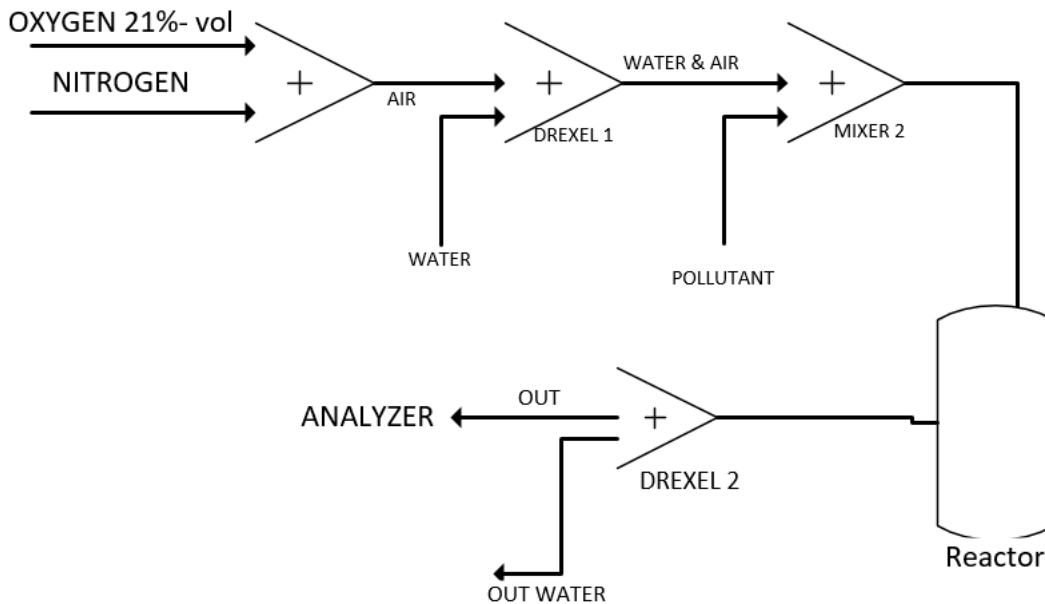


**Figure 4.2** Humidification plant of experiment tests.

The larger drexel was used in the phase of mixing water vapor and air: It was immersed in a container containing distilled water at a temperature of 65°C. The second one on the right, however, was used to condense the water, he too was immersed in a container containing water and ice.



**Immagine 4.3** on the left the Drexel of evaporation on the right the Drexel of condensation

## 4.5 Cyclic tests

In this phase of the study of the MnO<sub>2</sub> SCS catalyst, cyclic tests were conducted for the three molecules of CO, ethylene and propylene starting from a temperature of 25°C and reaching complete

conversion. The procedure involved, after assembling the reactor, a previous pre-treatment stage. A stream of nitrogen from a cylinder of 100ml/min was sent inside the quartz tube at a temperature of 160°C for approximately one hour, to desorb and "clean" the surface of the catalyst from molecules present. After having cooled the reactor and having prepared the mixture with 21% oxygen, 100ppm of pollutant and nitrogen to balance, the by-pass was closed. The first conversion cycle then began, at the end of which the bypass opened and the temperature decreased. Again, we started again with the pre-treatment and so on until the third cycle. As with the previous tests, the temperature and concentration of the exiting carbon dioxide were recorded, and the conversion was estimated using a balance sheet. All this was possible by assuming that the concentration of carbon dioxide arriving at the analyzer was deriving from the conversion of the pollutant molecule (minus that possibly present in the stream at room temperature).

## 5 Characterization results

### 5.1 Nitrogen physisorption at -196°C

In order to analyse the surface area, the pore structure of the commercial  $\text{MnO}_2$  and SCS samples, a nitrogen physisorption process was implemented at  $-196^\circ\text{C}$  and subsequently the data were processed according to the Brauner Emmett Teller method (BET). The figure 5.1 below show the adsorption and desorption isotherms of the samples  $\text{MnO}_2$  and  $\text{Mn}_2\text{O}_3$  commercial and SCS. From a qualitative analysis we can already obtain information on the nature of the material considered. From the data in the literature, it can be stated that these two materials are mesoporous in nature as the isotherms present the hysteresis phenomenon. As we can see, the desorption curve does not correspond to the adsorption one: during adsorption the gas molecules begin to fill the pore, forming a first layer and forming increasingly numerous layers. This leads to an instability of the gas phase which therefore, despite being at lower pressures than the saturation pressure, condenses and this can be noticed by the presence of the characteristic step. According to IUPAC, there is a second distinction, based on the shape of the isotherms. Graph (a), which refers to commercial  $\text{MnO}_2$ , shows a hysteresis that suggests the presence of interstitial pores caused by the presence of aggregates of sheet particles. In the case of commercial ones,  $\text{MnO}_2$  has an isotherm shifted downwards compared to  $\text{Mn}_2\text{O}_3$ , this is because the quantity of nitrogen adsorbed is smaller. In the case of catalysts synthesized with the SCS technique, a reversal of trend is noted and  $\text{MnO}_2$  SCS is better in terms of recovering the volume of physisorbed nitrogen.

The graph (b), which instead corresponds to  $\text{MnO}_2$  SCS, corresponds to the phenomenon of capillary condensation inside interstitial pores produced by the aggregation of particles.

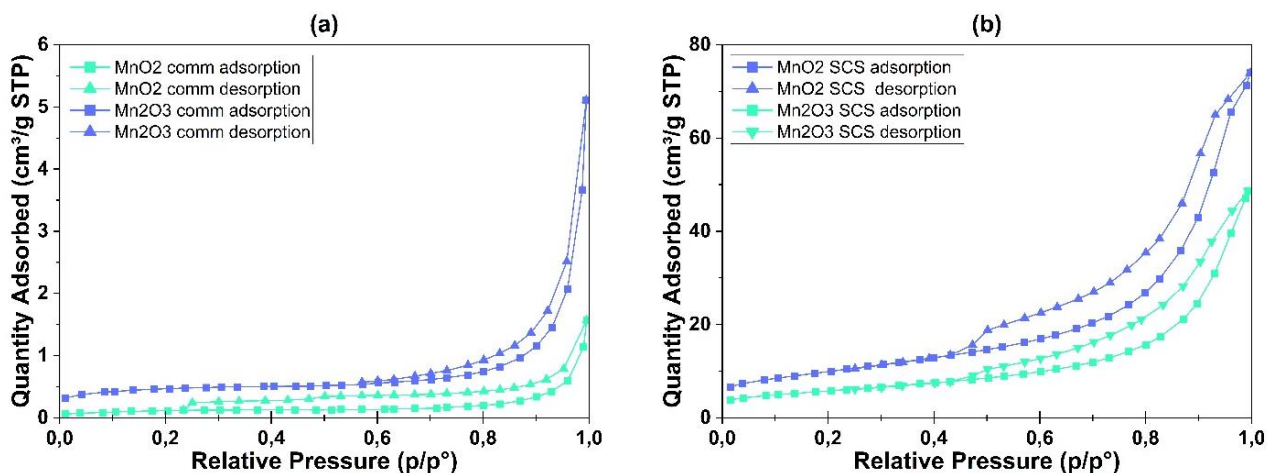


**Figure 5.1** (a) and (b) graphical representation of isotherms of  $\text{N}_2$  physisorption at  $-196^\circ\text{C}$  for commercial and SCS samples of  $\text{MnO}_2$  and  $\text{Mn}_2\text{O}_3$

The surface area is a parameter to consider as it is directly related to the porosity of our material, together with other quantities such as the specific volume and the distribution of the pore size (pore size distribution) it is fundamental to guarantee a certain surface activity and a certain adsorption volume. The specific area is defined as the ratio between the total surface area of the sample and its mass. On a practical level, an estimate of this total area can be obtained by considering the quantity of nitrogen that forms the first layer.

From Table 2 below it can be seen that the surface area is an order of magnitude higher for manganese oxides synthesized with the SCS technique, in particular MnO<sub>2</sub> SCS has the highest value of 35.7 m<sup>2</sup>/g, followed by manganese trioxide synthesized with the SCS technique and commercial ones. This therefore leads us to argue that, already in this first analysis, the MnO<sub>2</sub> SCS is more active compared to the remaining samples analysed.

**Table 2** Results of N<sub>2</sub> physisorption at -196°C calculated with BET method.

<b>Physisorption of N<sub>2</sub></b>	<b>Mn<sub>2</sub>O<sub>3</sub> comm</b>	<b>Mn<sub>2</sub>O<sub>3</sub> SCS</b>	<b>MnO<sub>2</sub> comm</b>	<b>MnO<sub>2</sub> SCS</b>
<b>Surface area (m<sup>2</sup>/g)</b>	1,6	20,1	0,4	35,7
<b>Total volume pore (cm<sup>3</sup>/g)</b>	0.007	0,075281	0,002	0,1
<b>Pore diameter (nm)</b>	20,3	14,5	23,2	12,8

As regards the size of the pores, the volume value is obtained by considering the total quantity of adsorbed nitrogen. In general, a material can be classified as micro, meso and macro depending on the diameter of the pores. Another information we can obtain is the average width of the pores. From the pore size distribution, obtained via the BJH method, we can see that for commercial MnO<sub>2</sub> the maximum is around 7 nm, while in the case of SCS the distribution presents a further peak at 17 nm for manganese dioxide.

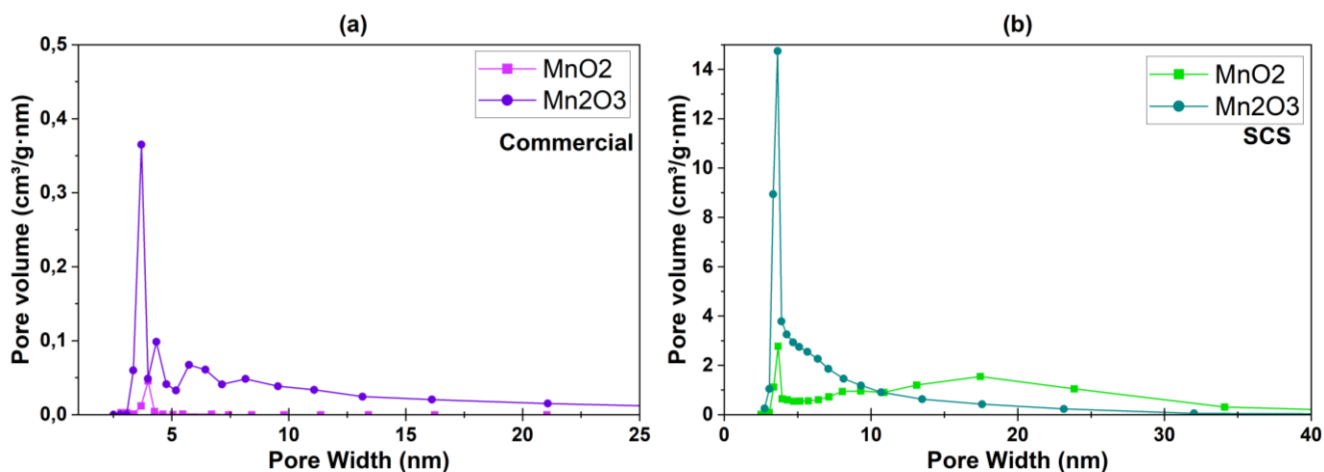


**Figure 5.2** (a), (b) graphical representation of the pore size distribution with BJH method (a) commercial MnO<sub>2</sub> and Mn<sub>2</sub>O<sub>3</sub>, (b) SCS MnO<sub>2</sub> and Mn<sub>2</sub>O<sub>3</sub>

## 5.2 X-Ray diffraction (XRD)

X-ray diffraction (XRD) is a characterization that determines the structure of the sample in a non-destructive way. We need to understand if there are phase transitions or possible preferential growth directions. Based on the shape of the diffractogram obtained it is possible to trace the type of material we are analysing. Through the patterns, three main pieces of information are obtained: peak profile, peak intensity and angular position. The profile and intensity allow us to consider the preferential orientation, structure and abundance of specific phases. The profile, however, is of essential importance for analysing the level of crystallinity and disorder of the sample. Using the High Score Plus software, it was possible to correlate the pattern with a specific type of material and its phase. From figure 5.4, we note that for SCS and commercial MnO<sub>2</sub> the diffraction peaks correspond, for both samples, to those of a tetragonal-type structure. This is Pyrolusite or  $\beta$ -type manganese (IV) dioxide. Pyrolusite is a mineral belonging to the rutile group. For both crystalline phases the diffractogram of the commercial is clearly more defined as the structure is perfectly crystalline, unlike that synthesized with the SCS technique. The degree of purity is 100% as there are no detectable peaks of other types of materials. As regards both SCS and commercial Mn<sub>2</sub>O<sub>3</sub>, they are Bixbiite C with a cubic-type crystallographic structure, also defined as  $\alpha$ -type Mn<sub>2</sub>O<sub>3</sub>. Also in this case, it is noted that the commercial one has a more crystalline and orderly structure compared to the counterpart synthesized with the SCS technique. The degree of purity is 100%. Figure 5.3 shows the images that refer to the CAD models of the MnO<sub>2</sub>  $\beta$  and  $\alpha$ -type Mn<sub>2</sub>O<sub>3</sub> crystalline structures.



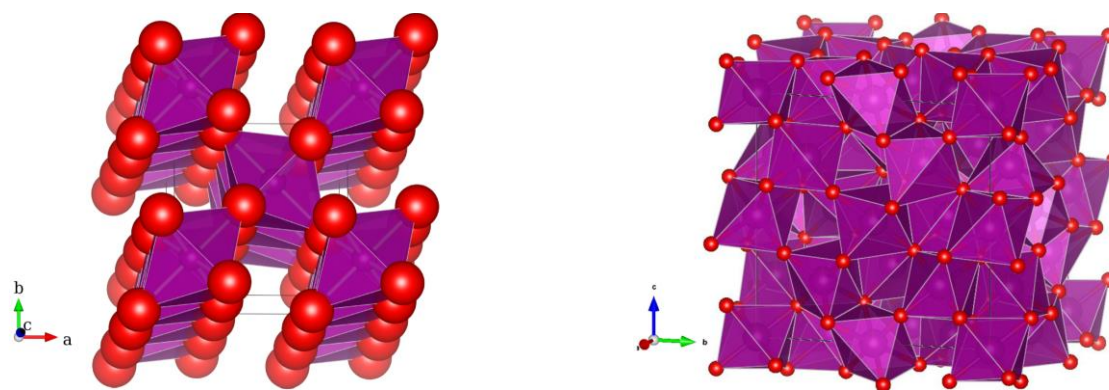


**Figure 5.3** Beta  $MnO_2$ , crystalline structure where the red spheres represent oxygens, while the purple octahedra represent manganese. (David A. Tompsett, 2014),  $Mn_2O_3$  cubic structure (R. Nikam, 2017)

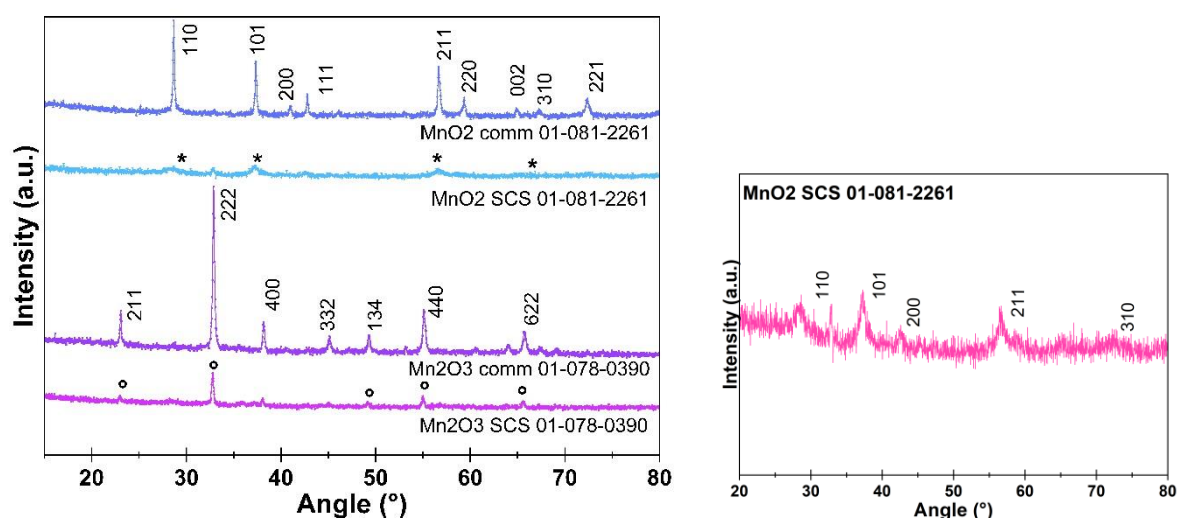


**Figure 5.4** Diffraction pattern of  $MnO_2$  and  $Mn_2O_3$  SCS and commercial with a zoom on  $MnO_2$  SCS

Let us now consider a second piece of information obtainable through X-ray diffractometry: crystallites. The crystalline grain, or crystallite, is a characteristic crystal structure or orientation common to a certain portion of the powder, and the size and orientation of these is directly related to the synthesis method and the thermal history of the material. An estimate of the crystallite size was obtained using the Scherrer equation. It allows us to correlate the size of the sub-micrometric crystalline domains to the width of the diffraction peak (FWHM). As we can see in Table 2, the crystallites of the  $MnO_2$  SCS sample are smaller than the others. A smaller size of the crystallites indicates that the order of the crystal lattice is more often lacking and consequently it presents a greater quantity of lattice defects. These defects profoundly influence the physical and mechanical properties of the material. In the specific case of catalysts, a greater presence of defects is a sought-after quality as it determines greater activity of the material.

**Table 3** Crystallites dimension

<b>Crystallites dimensions (nm)</b>	
MnO <sub>2</sub> SCS	7
MnO <sub>2</sub> commercial	153
Mn <sub>2</sub> O <sub>3</sub> SCS	37
Mn <sub>2</sub> O <sub>3</sub> commercial	136

### 5.3 Photoelectron spectroscopy with X ray(XPS)

X-ray photoelectric spectroscopy (X-ray photoelectron spectroscopy) allows the chemical species present on the surface of the sample and their oxidation state to be determined through the interaction of the radiation with the matter. This technique uses X-rays which have an energy between 200 and 2000 eV, which bombard the surface of the material and the kinetic energy emitted by the electrons is consequently measured. This is a particularly sensitive technique (around 10 nm), capable of detecting the oxidation number of elements. It can detect all chemical elements except helium and hydrogen. Figure 5.4 shows the deconvolution of the O1s and Mn2p spectra of the SCS and commercial MnO<sub>2</sub> and Mn<sub>2</sub>O<sub>3</sub> samples. Two species of oxygen are present on the surface of the catalyst, generally  $\alpha$  and  $\beta$ . The former are only chemisorbed, that is, they have formed a stable bond with the metal molecule and consequently have a fair amount of mobility. The latter, however, become part of the actual crystalline lattice and are not as available to participate in certain oxidation reactions. Furthermore, the  $O_{\alpha}$  ones are more electrophilic than the  $O_{\beta}$  ones and give rise to complete oxidation reactions with the elements they encounter, while the  $O_{\beta}$  ones are the source of more selective reactions. They are characterized by a different level of bond energy, and this makes their recognition possible. An estimate of their ratio is essential to evaluate the activity of the material. A greater presence of  $O_{\alpha}$  oxygens make the material more active and capable of converting the molecules with which it comes into contact more quickly.

In general, it can be stated that the signal between 529.7-530.1eV refers to  $O_{\beta}$  ( $O^{2-}$ ). Instead, the 531.1-531.7 eV signal refers to  $O_{\alpha}$  oxygens. (Kaushik Natarajan, 2018)

Table 3 shows the ratios of  $O_{\alpha}/O_{\beta}$ . As we can see by comparing the percentage values of  $O_{\alpha}/O_{\beta}$  for MnO<sub>2</sub> SCS compared to the commercial one we have a greater presence of  $O_{\alpha}$ . The same goes for Mn<sub>2</sub>O<sub>3</sub>.

MnO <sub>2</sub> SCS	52%
MnO <sub>2</sub> commercial	40%
Mn <sub>2</sub> O <sub>3</sub> SCS	33%
Mn <sub>2</sub> O <sub>3</sub> commercial	20%

As regards the Mn2p spectrum, the peaks between 641 and 643 eV refer to the oxidation states +2, +3, +4. The Mn<sup>2+</sup> sites are tetrahedral in shape while the Mn<sup>3+</sup> ones are octahedral. (Alain Manceau, 1992)

As regards the Mn2p spectrum, this is generally divided into two sections Mn2p<sub>1/2</sub> and Mn2p<sub>3/2</sub>. Three types of ions can be present on the surface of a manganese-based oxide, depending on their oxidation state: Mn<sup>2+</sup>, Mn<sup>3+</sup>, Mn<sup>4+</sup>, whose binding energies are in the range 641-643 eV. In general, a greater quantity of Mn<sup>4+</sup> ions determines a positive effect on the sample as it will have a greater tendency to reduce at low temperatures compared to other ions. (Deng, 2016)

The Mn<sup>2+</sup> sites are tetrahedral in shape while the Mn<sup>3+</sup> sites are octahedral. (Alain Manceau, 1992). Mn<sup>2+</sup> has a binding energy that is around 640.5 and 640.8 eV, Mn<sup>3+</sup> between 641.9 and 642.1 eV and Mn<sup>4+</sup> between 643.3 and 643.8 eV.

Table 4 shows the percentage values of the various Mn<sup>2+</sup>, Mn<sup>3+</sup>, Mn<sup>4+</sup> ions with the relative binding energies. MnO<sub>2</sub> SCS presents the highest concentration of Mn<sup>4+</sup> species, this determines a greater reducibility of the sample confirmed by the H<sub>2</sub>-TPR tests, as we are gonna discuss later. The commercial MnO<sub>2</sub> and Mn<sub>2</sub>O<sub>3</sub> have a high concentration of Mn<sup>2+</sup> ions. This tends to disadvantage their reducibility.

**Table 5** percentages of manganese ions present on the surface of samples and relative binding energy and ratios.

	BE	Mn <sup>2+</sup>	BE	Mn <sup>3+</sup>	BE	Mn <sup>4+</sup>	Mn <sup>4+</sup> / Mn <sup>3+</sup>	Mn <sup>3+</sup> / Mn <sup>2+</sup>
<b>Mn<sub>2</sub>O<sub>3</sub> comm</b>	640,8	76,3	641,5	17	643,3	7,7	0,41	0,22
<b>Mn<sub>2</sub>O<sub>3</sub> SCS</b>	641,7	73,2	642,1	20,8	643,5	6	0,29	0,28
<b>MnO<sub>2</sub> comm</b>	641,5	89,6	642,5	14	643,4	6,4	0,40	0,16
<b>MnO<sub>2</sub> SCS</b>	641,1	49,4	642,5	35	643,3	15,6	0,45	0,61

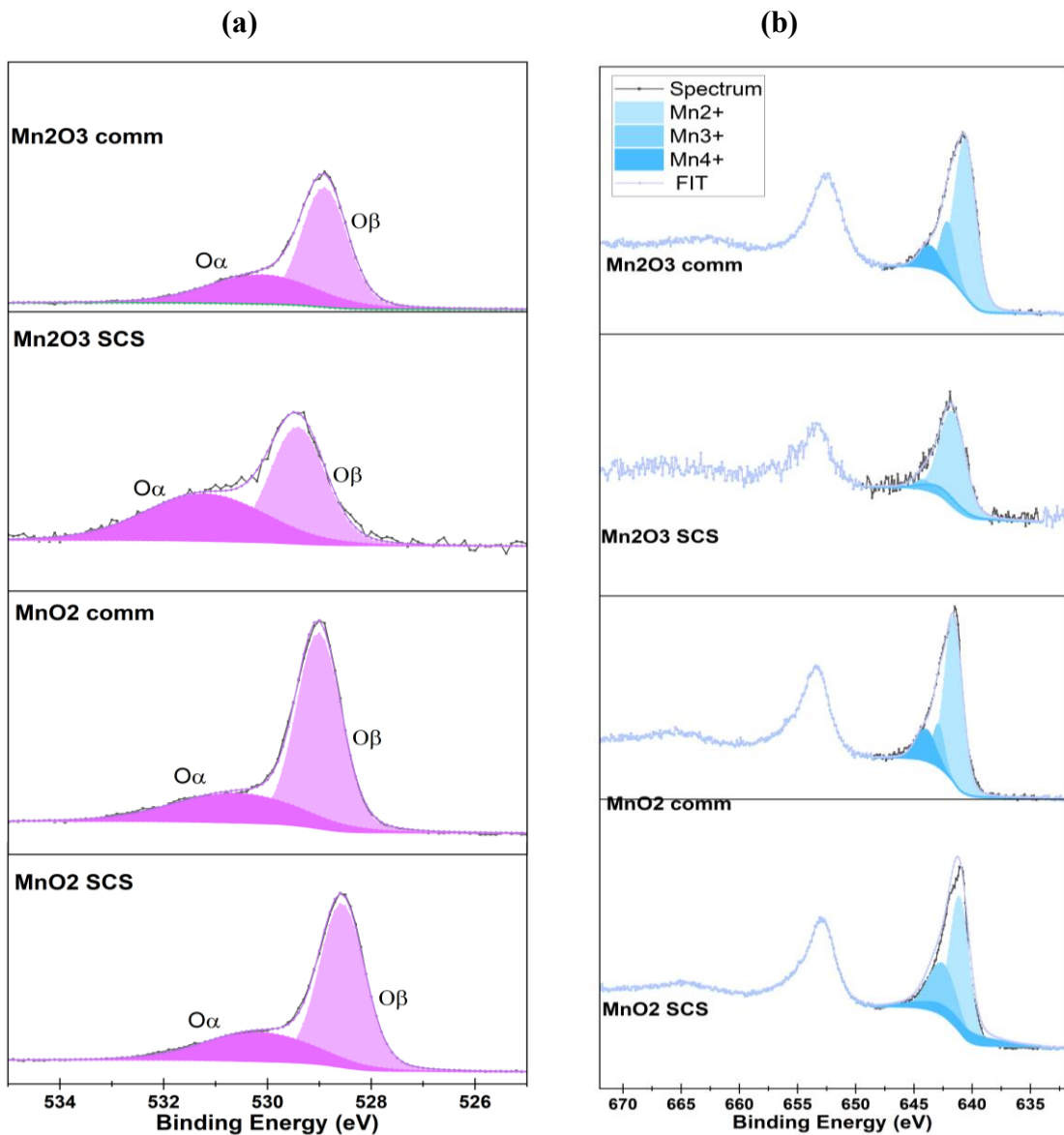


**Figure 5.5** (a) XPS spectra of samples O1s (b) XPS spectra of samples Mn2p

#### 5.4 Programmed temperature reduction with hydrogen ( $H_2$ -TPR)

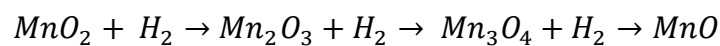
The objective is to obtain a hydrogen consumption defined as [mmol/g<sub>cat</sub>]. Through a thermal conductivity detector (TCD) it is possible to trace the presence of reduction reactions. The peak temperature is characteristic of the material and is related to the reactivity of the species present on the surface of the catalytic powder.

From figure 5.6 we can observe that both manganese oxides present two peaks: MnO<sub>2</sub> commercial at higher temperatures (360, 540°C) compared to those of the SCS (310, 410°C). The manganese reduction process can be generalized as follows: (Katpteijin et al, 1994)

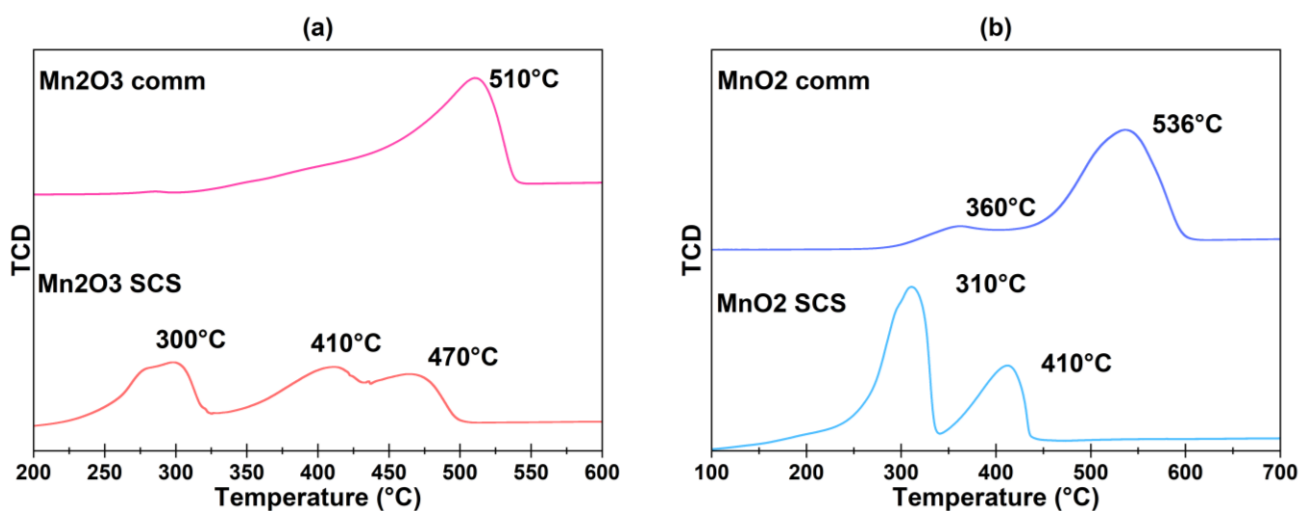
The first peaks, therefore, would attest to the reduction of manganese dioxide to manganese trioxide, therefore passing from an oxidation state +4 to an oxidation state +3, the second peak instead from +3 to +2.

Table 5 is shown below with the hydrogen consumption normalized with respect to the mass of sample used and the related peak temperatures. In order to calculate the area of the curves, the ORIGIN® software was used. These experimental consumptions are compared with the theoretical ones obtained considering MnO as the final oxidation stage.

From the figure we can observe that both manganese oxides present two peaks: MnO<sub>2</sub> commercial at higher temperatures (360, 540°C) compared to those of the SCS (310, 410°C). The manganese reduction process can be generalized as follows: (Katpteijin et al, 1994)



The first peaks, therefore, would attest to the reduction of manganese dioxide to manganese trioxide, therefore passing from an oxidation state +4 to an oxidation state +3, the second peak instead from +3 to +2.



**Figure 5.6** H<sub>2</sub>-TPR profiles of MnO<sub>2</sub> and Mn<sub>2</sub>O<sub>3</sub> commercial e SCS

Below is table 4 with the hydrogen consumption, normalized for the quantity of sample considered, for the two different catalysts used at the temperatures corresponding to the peaks. In order to calculate the area of the curves, the ORIGIN® software was used. These experimental consumptions are then compared with the theoretical ones obtained considering MnO as the final oxidation stage.

To obtain the calibration factor, copper oxide was used which oxidizes according to the following reaction:



The theoretical consumption of  $\text{MnO}_2$ , the value is equal to 11.5 mmol/g<sub>cat</sub>, while for  $\text{Mn}_2\text{O}_3$ , it is equal to 6.33 mmol/g<sub>cat</sub>. This data was used during the processing phase to understand which of the various samples was the best. The closer the hydrogen consumption is to the theoretical one, the better its reduction capacity. At the same time, the peak temperature must be considered: the lower the peak temperature the greater the activity of the material at lower temperatures. In figure 5.5, Mn catalysts are shown in (a) while both commercial and SCS  $\text{MnO}_2$  are shown in (b).

In (a) we note how the commercial presents a single peak at a temperature of 510°C, with an on-set at around 300°C, corresponding to a gradual reduction process from  $\text{Mn}^{3+}$  to  $\text{Mn}^{2+}$ . While the SCS type presents two peaks, one of which is asymmetrical at a temperature between 300°C for the first and 400°C-500°C for the second. This is why we can say that SCS is better than the commercial type. In graph (b) however we see how the commercial type has two peaks like SCS but at higher temperatures, in both cases the peaks refer to the reduction from  $\text{Mn}^{4+}$  to  $\text{Mn}^{3+}$  and from  $\text{Mn}^{3+}$  to  $\text{Mn}^{2+}$ . In table 4 we see how the best, in terms of consumption and temperature range, is  $\text{MnO}_2$  SCS, the first peak is around 300°C corresponding to the reduction of  $\text{MnO}_2$  to  $\text{Mn}_2\text{O}_3$  and the total hydrogen consumption is very close to that theoretical.

SCS and commercial  $\text{Mn}_2\text{O}_3$  have a hydrogen consumption higher than the theoretical one calculated, this leads us to think that both  $\text{Mn}^{4+}$  and  $\text{Mn}^{3+}$  ions are present on the surface and that both undergo a reduction process. (Clarissa Cocuzza, 2023)

**Table 6** Normalized catalyst hydrogen consumption with relative peak temperatures.

<b>H2-TPr</b>	<b>Temperature range (°C)</b>	<b>mmol/g<sub>cat</sub></b>
<b>MnO<sub>2</sub> SCS</b>	300-310	8,2
	400-410	3,5
<b>MnO<sub>2</sub> comm</b>	350-400	0,4
	500-550	5,1
<b>Mn<sub>2</sub>O<sub>3</sub> SCS</b>	300-310	2,6
	400-410	2,5
	450-500	1,8
<b>Mn<sub>2</sub>O<sub>3</sub> comm</b>	600	8

## 5.5 Temperature programmed desorption of oxygen ( $O_2$ -TPD)

In order to analyse the mobility of the oxygens present on the surface of the catalytic powder, the  $O_2$ -TPD technique, the temperature-controlled desorption of oxygen, was used.

Also in this case, as for the TPR, a pre-treatment in a helium stream was carried out with a flow of 40 ml/min for hours at a temperature of 800°C. The desorption process instead expected to reach a temperature of 850°C.

In the literature, lattice oxygens are classified as  $\alpha$ ,  $\beta$ ,  $\gamma$ . Depending on the strength of the oxygen and manganese bond. In general, when manganese is characterized by a +4 oxidation state then the lattice oxygens are classified as  $\gamma$  type.

In general, we observe three peaks, the first of which is particularly easy to recognize. For commercial manganese dioxide the peak is found at a temperature of around 600°C while for the SCS type it is at a temperature lower than 525°C, demonstrating that this is less stable. The oxygens of the  $MnO_2$  SCS lattice can therefore be considered more reactive as the bond is more labile. (V.P. Santos, 2010)

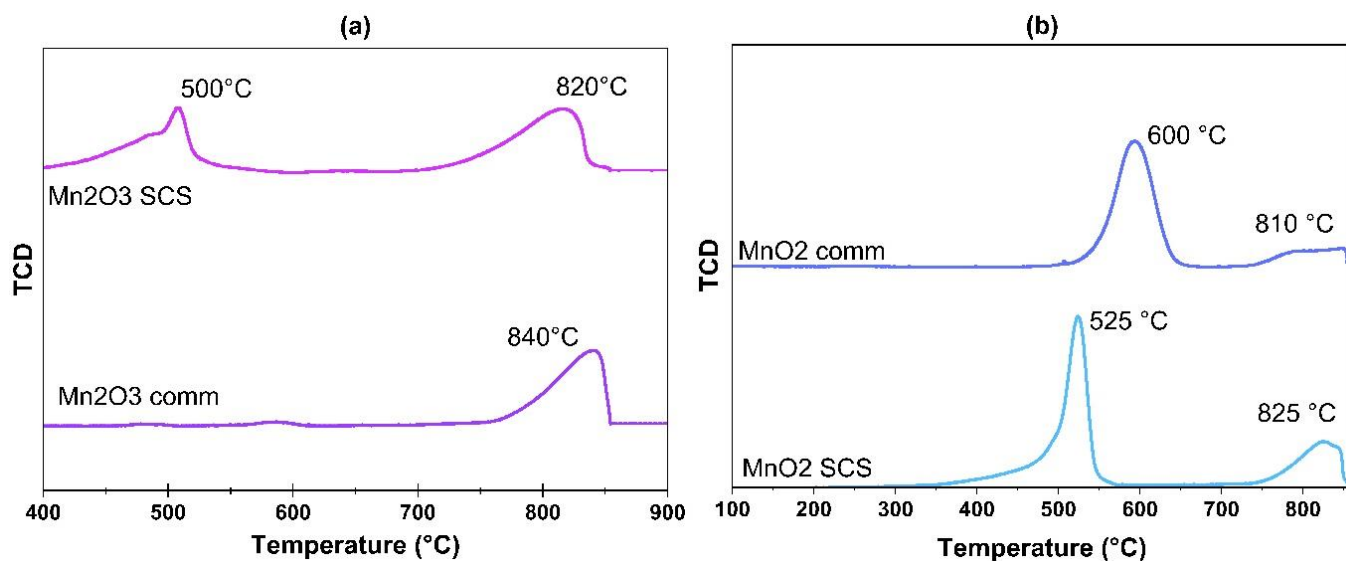


Figure 5.7  $O_2$ -TPD dei campioni di  $MnO_2$  e  $Mn_2O_3$  commerciale e SCS

The following results of desorption are reported.

**Table 7** Dati di desorbimento specifico di ossigeno per i catalizzatori

$O_2$ - TPD	Temperature range (°C)	$mmol/g_{cat}$
$MnO_2$ SCS	500-550	0,6
	>800	0,1
$MnO_2$ comm	600-650	0,6
	>800	0,2
$Mn_2O_3$ SCS	500-550	0,1
	>800	0,2

## 5.6 FESEM results

Figure 5.8 shows the images of the surfaces of the  $MnO_2$  and  $Mn_2O_3$  samples synthesized with the SCS technique (a) and (b) respectively. As can be seen, the surface of the  $MnO_2$  SCS sample has tetragonal-shaped crystals as found by X-ray diffactometry. In (b) however, the cubic-type crystals typical of  $\alpha$ -type  $Mn_2O_3$  can be seen.

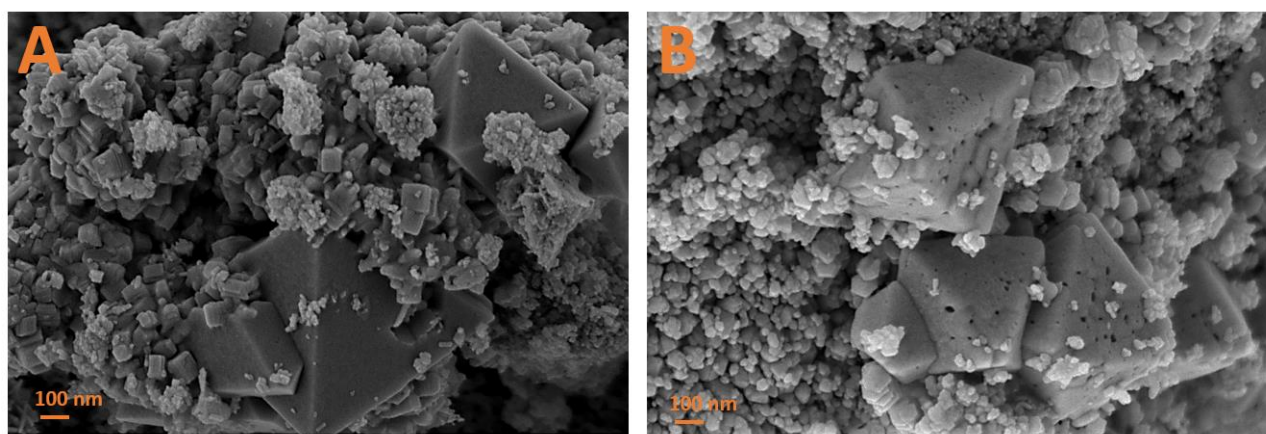


**Figure 5.8** FESEM images of catalyst surface (a)  $MnO_2$  SCS and (b)  $Mn_2O_3$  SCS



## 6 Tests Results

### 6.1 Dry tests results

In this first phase of experimental tests, the performance of the catalyst in standard conditions was analyzed. The following graphs show the comparison between  $\text{MnO}_2$  and  $\text{Mn}_2\text{O}_3$  both commercial and synthesized with the SCS technique and blank. The use of a catalyst accelerates the reaction speed in any case: in fact the conversions in the absence of these solids are equal to zero for carbon monoxide and below 10% in the case of ethylene and propylene at temperatures of  $300^\circ\text{C}$ , at the limits we had pre-established.

For all three molecules, a clear improvement in the performance of  $\text{MnO}_2$  SCS was noted compared to the others. In figure (a) for carbon monoxide, as we note, the trend of the curve of commercial  $\text{MnO}_2$  and  $\text{Mn}_2\text{O}_3$  commercial type overlap, while  $\text{Mn}_2\text{O}_3$  SCS completely covers at  $275^\circ\text{C}$ .  $\text{MnO}_2$  SCS, on the other hand, allows for 100% conversion at  $125^\circ\text{C}$ , just under half. In figure (b) which refers to the commercial ethylene molecule  $\text{MnO}_2$  is better than the  $\text{Mn}_2\text{O}_3$  phase. In presence of  $\text{MnO}_2$  SCS the ethylene is completely converted into  $\text{CO}_2$  at  $225^\circ\text{C}$ , a lower temperature than in presence of  $\text{Mn}_2\text{O}_3$  SCS.

In summary,  $\text{MnO}_2$  SCS allows you to convert 100 ppm of pollutant at  $120^\circ\text{C}$  for carbon monoxide,  $225^\circ\text{C}$  for ethylene and  $175^\circ\text{C}$  for propylene. The fact that  $\text{MnO}_2$  SCS is more active than the other catalysts considered is since, as was established during the characterization phase, it has better qualities from many points of view. First, the greater specific area and smaller size of the crystallites are present, which means a greater quantity of active sites due to the presence of greater lattice defects. It has a higher percentage of alpha oxygens which, unlike betas, are more mobile and react more easily. Finally, the TCD profiles as a function of temperature demonstrated that  $\text{MnO}_2$  had greater reducibility and a greater quantity of desorbed oxygens at significantly lower temperatures compared to the other samples.

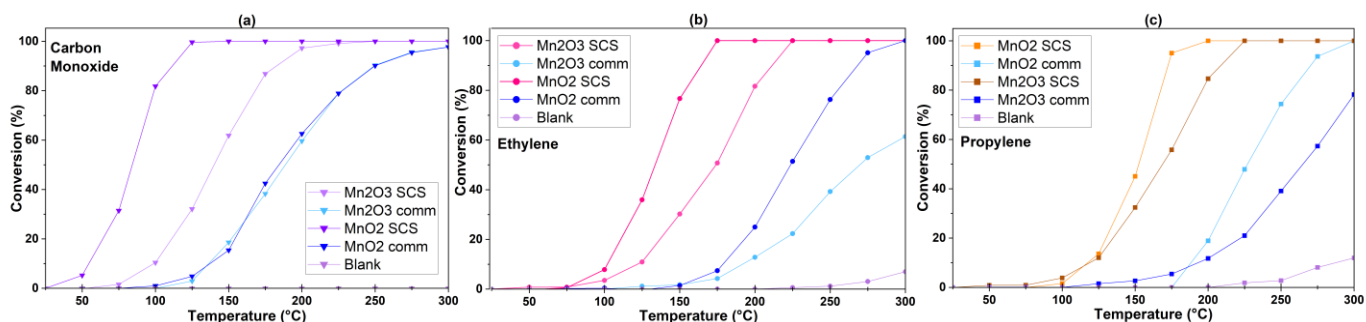


**Figure 6.1 (a),(b), (c)** Carbon Monoxide, Ethylene, Propylene oxidation confrontation among blank, MnO<sub>2</sub> and Mn<sub>2</sub>O<sub>3</sub> commercial and SCS in dry condition, 50 mg of catalyst.

Below are the conversion temperatures of 10%, 50% and 90% for the different samples considered. Also, in this case we can state that MnO<sub>2</sub> SCS is more active at lower temperatures than other catalysts.

**Table 8** Temperature conversion for Carbon Monoxide

	Mn <sub>2</sub> O <sub>3</sub> SCS	Mn <sub>2</sub> O <sub>3</sub> commercial	MnO <sub>2</sub> SCS	MnO <sub>2</sub> commercial
<b>T<sub>10%</sub> (°C)</b>	99	136	54	137
<b>T<sub>50%</sub> (°C)</b>	140	189	89	184
<b>T<sub>90%</sub>(°C)</b>	183	248	111	250

**Table 9** Temperature conversion for Ethylene

	Mn <sub>2</sub> O <sub>3</sub> SCS	Mn <sub>2</sub> O <sub>3</sub> commercial	MnO <sub>2</sub> SCS	MnO <sub>2</sub> commercial
<b>T<sub>10%</sub> (°C)</b>	119	188	118	193
<b>T<sub>50%</sub> (°C)</b>	162	227	131	265
<b>T<sub>90%</sub> (°C)</b>	224	<300	208	<300

**Table 10** Temperature conversion for Propylene

	Mn <sub>2</sub> O <sub>3</sub> SCS	Mn <sub>2</sub> O <sub>3</sub> commercial	MnO <sub>2</sub> SCS	MnO <sub>2</sub> commercial
<b>T<sub>10%</sub> (°C)</b>	122	192	102	179
<b>T<sub>50%</sub> (°C)</b>	174	270	134	224
<b>T<sub>90%</sub> (°C)</b>	211	<300	160	268

**Table 11** Rates of the considered molecules the catalyst of  $Mn_2O_3$  and  $MnO_2$  commercial have been excuded because of their inactivit at the chosen tempertures

	Temperature	$Mn_2O_3$ SCS (nmol/h/m <sup>2</sup> )	Conversion	$MnO_2$ SCS (nmol/h/m <sup>2</sup> )	Conversion
CO	75°C	0,6	2%	6,2	31%
Ethylene	125°C	2,8	12%	3	14%
Propylene	125°C	4,4	12%	7,1	36%

## 6.2 Humid Tests

The three graphs in the figure 6.2 show respectively the conversion of carbon monoxide, ethylene and propylene molecules in the presence of  $MnO_2$  SCS in dry and wet conditions and the blank in the presence of humidity. The curves are shifted to the right by approximately 50°C. For carbon monoxide, complete conversion is achieved at 175°C, at 250°C for ethylene and at 225°C for propylene. The presence of water vapor within the stream to be converted causes an effective reduction in the performance of the catalyst. This is because when the pollutant mixture meets the surface of the catalyst, not only the pollutant molecules will be involved in an adsorption phenomenon on the catalytic site, but also the water molecules which, however, will not react they will only represent a physical obstacle. In this case the graphs show the comparison between the conversions of  $MnO_2$  SCS in dry conditions and in wet conditions and the blank in wet conditions. Therefore, to have the same conversion, in the presence of humidity, higher temperatures will be required as shown by the experimental test. Despite this,  $MnO_2$  SCS allows a complete conversion of all three molecules to be achieved at temperatures below 300°C. This is due to the fact that  $MnO_2$  SCS, unlike the other catalysts considered, has a greater specific area and therefore a greater presence of active sites for the oxidation reaction. The water inside the system will occupy a fair part but not all of it.

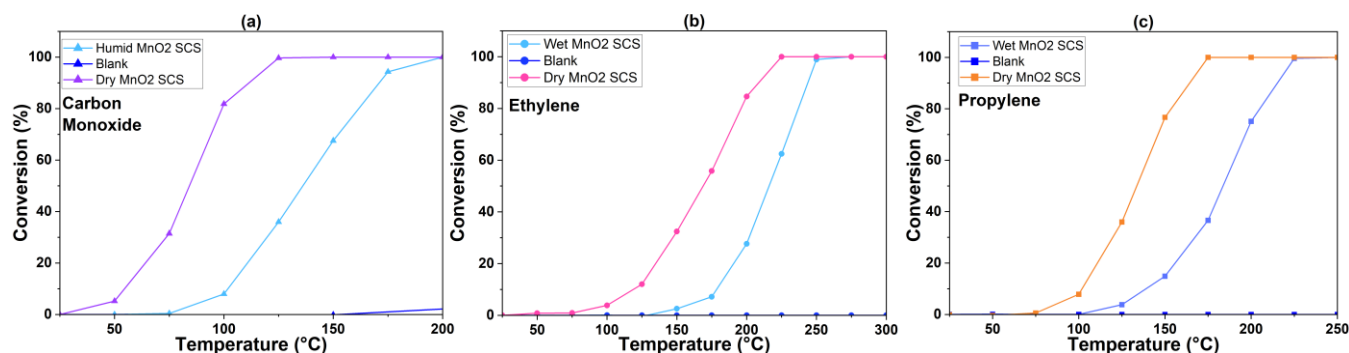


**Figure 6.2** (a), (b), (c) Carbon monoxide, Ethylene and Propylene oxidation confrontation in presence of  $MnO_2$  commercial, SCS and in blank condition, 50 mg of catalyst and RH 10%

**Table 12** temperature conversion of carbon monoxide in wet and dry conditions

	<b>WET</b>	<b>DRY</b>
<b>T<sub>10%</sub> (°C)</b>	102	55
<b>T<sub>50%</sub> (°C)</b>	136	89
<b>T<sub>90%</sub> (°C)</b>	171	111

**Table 13** temperature conversion of ethylene in wet and dry conditions

	<b>WET</b>	<b>DRY</b>
<b>T<sub>10%</sub> (°C)</b>	180	122
<b>T<sub>50%</sub> (°C)</b>	221	174
<b>T<sub>90%</sub> (°C)</b>	257	211

**Table 14** temperature conversion of propylene in wet and dry conditions

	<b>WET</b>	<b>DRY</b>
<b>T<sub>10%</sub> (°C)</b>	139	102
<b>T<sub>50%</sub> (°C)</b>	184	134
<b>T<sub>90%</sub> (°C)</b>	215	121

### 6.3 Tests on the catalytic performance in time

There are countless factors that affect the stability of a catalyst such as thermal degradation, poisoning, fouling and finally aging. In this test phase, the performance of the catalyst was analysed in relation to the time of use, according to two methods: cyclic tests and time on stream tests. The first analyses whether there are significant conversion changes as the number of cycles to which the catalyst is subjected increases. The second, however, aims to analyse its capabilities for longer periods of time and at higher operating temperatures.

#### 6.3.1 Cyclic tests

Below are graphs in the figure 6.3 in (a),(b),(c) of carbon monoxide, ethylene and propylene molecules. As can be seen, the complete conversion of CO and propylene molecules occurs at lower temperatures than those of ethylene (140°C, 160°C, 210°C respectively). The conversion curves are superimposed in all three cases, demonstrating the stability of the MnO<sub>2</sub> SCS catalyst.

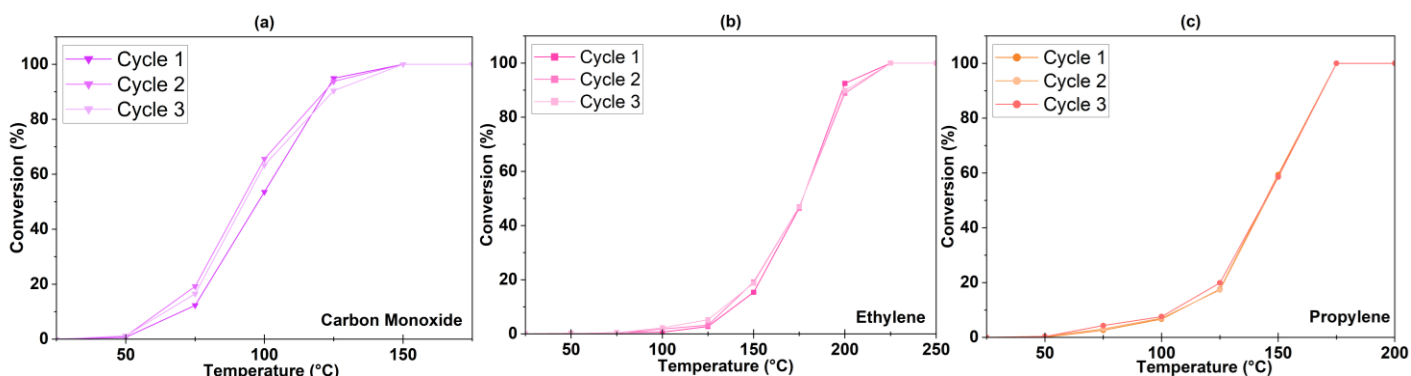


**Figure 6.3** (a), (b), (c) Cyclic tests of carbon monoxide, ethylene and propylene in presence of 50 mg of MnO<sub>2</sub> SCS, each test has been repeated 3 times.

### 6.3.2 Time on stream tests

TOS are carried out both in the presence and absence of water vapour. In dry conditions, the test was carried out both with fresh catalyst figure 6.4 and after having undergone three conversion cycles, therefore no longer fresh, figure 6.5.

In figure 6.4 we observe the conversion with fresh MnO<sub>2</sub> SCS and the conversion remains stable for all three molecules. In (a) we observe that the conversion remains at an average value of 92.4% for all eight hours. For ethylene and propylene, (b) and (c) respectively, there is a slight drop in conversion after approximately four hours for ethylene and after two hours for propylene. In particular, in the case of ethylene the conversion decreases from around 90% to almost 85%. In the case of propylene, however, there is a peak at 90% and then decreases quite suddenly and stabilizes at an average value of 80%. This phenomenon may be related to the consequent capping of some active sites by the pollutant molecules or by the CO<sub>2</sub> molecules produced which do not free the active site once formed. In this case, therefore, a regeneration process at high temperatures would be necessary.

As for the non-fresh MnO<sub>2</sub> SCS catalyst. As we can see from the graphs in figure 6.5 (a), (b), (c) which refer to the molecules of CO, ethylene and propylene, the conversion remains stable. These graphs refer to catalysts that had already undergone three conversion cycles, so they could not be considered actually fresh. In particular, the conversion of carbon monoxide remains constant throughout the eight hours at a value of 83%. For the ethylene molecule, a temperature of 210° C was chosen, which corresponded to a conversion of approximately 94%. We can see how the catalyst reacts well in the first four hours, maintaining a constant conversion trend, and subsequently, there is a slight decrease, and the conversion drops to approximately 87%. For the propylene molecule we see a slow decrease in conversion which goes from 80% at the beginning of the test to almost 73%

towards the end. This phenomenon may be related to the consequent capping of some active sites by the pollutant molecules or by the CO<sub>2</sub> molecules produced which do not free the active site once formed. In this case, therefore, a regeneration process at high temperatures would be necessary.

In figure 6.6, TOS type tests were conducted in conditions of relative humidity of 10%. In this case, in order to maintain the conversion close to a value of 90%, the operating temperature had to be increased: 175°C for carbon monoxide, 240°C for ethylene and 215°C for propylene. Excellent results were obtained for carbon monoxide whose conversion remains stable for the entire duration of the cycle. For ethylene and propylene molecules, however, it is noted that the presence of water affects the stability of the catalyst in converting pollutants to CO<sub>2</sub>. It is noted that the conversion fluctuates around 90%, stabilizing only in the last test phase. This may be since the system, in the presence of water vapor, needed more time to reach a steady state phase compared to dry conditions. Despite this, there is no drastic drop in performance, therefore we can state that the catalyst is considered stable.

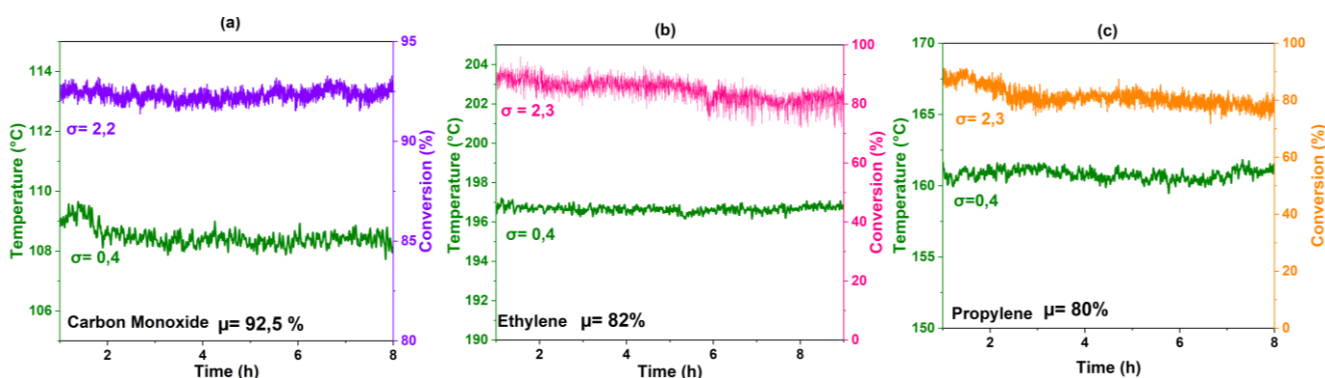


**Figure 6.4** TOS of Carbon Monoxide(a), Ethylene (b), Propylene (c) at 110°C for 8 hours with a conversion near between 80-90% at constant temperature: for CO 110°C, for Ethylene 210°C, for Propylene 160°C.

**Table 15** standard deviation and medium value of TOS in dry condition for fresh MnO<sub>2</sub> SCS

Molecule	Mean Conversion (%)
Carbon Monoxide	92,5%
Ethylene	82%
Propylene	80%

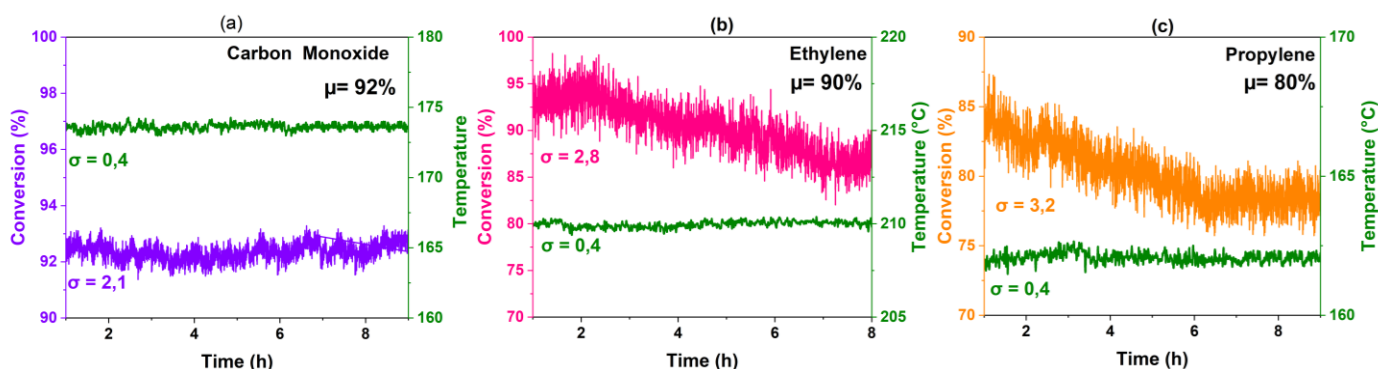


**Figure 6.5** TOS of Carbon Monoxide(a), Ethylene (b), Propylene (c) at 110°C for 8 hours with a conversion near between 80-90% at constant temperature: for CO 110°C, for Ethylene 210°C, for Propylene 160°C.

**Table 16** mean value of conversion for carbon monoxide, ethylene and propylene

Molecule	Mean Conversion (%)
Carbon Monoxide	92%
Ethylene	90%
Propylene	80%
Molecule	Mean Conversion (%)
Carbon Monoxide	92%
Ethylene	80%
Propylene	90%
Molecule	Mean Conversion (%)
Carbon Monoxide	92%
Ethylene	80%
Propylene	90%

The figure shows the TOS of the same molecules in the presence of humidity. The catalyst, in this case, the MnO<sub>2</sub> SCS catalyst used is completely fresh. In the case of carbon monoxide, we can see that the conversion remains perfectly constant throughout the eight hours of testing. In this case, in the presence of water vapor from the stream, the operating temperatures are higher than in dry conditions: for carbon monoxide 174°C, for ethylene 240°C and propylene 215°C. For the carbon monoxide shown in figure (a) we see how the conversion remains stable for all eight hours of testing with a standard deviation of 2,1 and an average value that stands around 92% .

For ethylene and propylene, (b) and (c), it is noted that in the first test phase the system reaches a maximum conversion above 90% and then decreases and stabilizes at an average conversion value equal to 80% for ethylene and 90% for propylene. This phenomenon may be due to the system needing more time to reach stationary. The presence of water would therefore also represent a slowdown from a time point of view for the system.

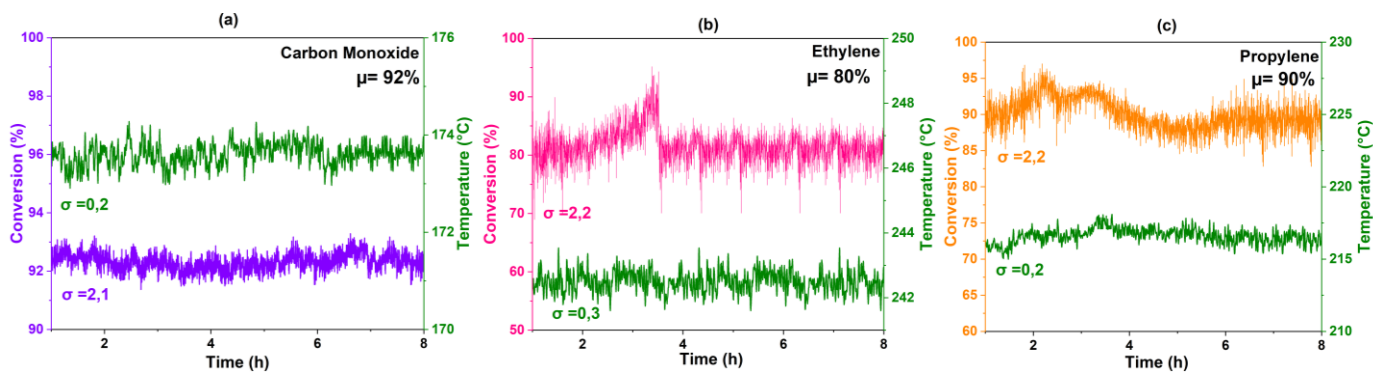


**Figure 6.6** (a), (b), (c) TOS of Carbon monoxide, Ethylene and Propylene in wet condition, 50 mg of fresh MnO<sub>2</sub> SCS

**Table 17** mean value for TOS in wet condition in presence of MnO<sub>2</sub> SCS

Molecule	Mean Conversion (%)
Carbon Monoxide	92%
Ethylene	80%
Propylene	90%

## 6.4 Test for replicability

### 6.4.1 Replicability and reproducibility

At the basis of the modern scientific method of the 20th century, the philosopher Karl Popper argued that a fact that occurred only once cannot be considered of scientific relevance. In the catalysis sector the problem of reproducibility influences every single step starting from the synthesis up to the testing phases. The problem of replicability and reproducibility, in addition to hindering researchers on a practical level, can also lead to erroneous considerations on the understanding of the most complex catalytic phenomena. Homogeneous catalysis is less affected by the risk of irreproducibility unlike heterogeneous catalysis. In this specific sector, in fact, the use of amorphous materials characterized by the presence of numerous crystalline defects, minor molecular species or active sites can be the cause of most of the catalytic activity observed. (Schweitzer, 2022)



Reproducibility and replicability are two different topics of statistical analysis. The reproducibility is the successful reproduction of the original data by independent reanalysis by using the identical approach of analysis. Consequently, to guarantee the reproducibility of the data, the replicability of the data that the operator has obtained must be guaranteed. For this reason, each experimental phase must be carefully described and monitored. The precise control of the operating conditions (such as concentrations, temperature, flow rates etc.) allow reliable data to be obtained. According to Susannah L. Scott's article, (Susannah L. Scott, 2022) a conversion difference of +/-10% does not represent a change in catalytic activity. It must be taken into consideration that during a catalytic process the transport of heat and mass heavily influences the performance, especially about nanostructured materials. In this case, factors such as pore size, reactor configuration and particle size must be known. To be able to bring them back into the search. In this way the researcher who wants to delve deeper into the topic will use similar values. For this reason, a fair amount of diligence and a good amount of time is required in the description phase of each single step of the experimental phase. (Susannah L. Scott, 2022)

The replicability, instead, is finding the same or very similar results using a new sample. It involves all contributions to the uncertainty of a measurement involving operators, materials, and equipment. It is related to the concepts of repeatability and replicability and represents a fundamental basis of the scientific method. It allows, later, to obtain similar measurements from different operators at different time with a high degree of authenticity making possible to deepen the research. (Susannah L. Scott, 2022)

## 6.4.2 Tests results

In figure 6.7, it is possible to visualize the overlapping of the conversion curves, corroborating the reproducibility of the results. The deviation value never exceeded 5% from the average of the values obtained. For this reason the results can be considered reproducible.

Consequently, we considered the standard deviation for the conversions at different temperatures, obtaining the graph in the figure for the three molecules.

$$\sigma = \sqrt{\frac{\sum_i (x_i - \mu)^2}{N}} \quad \text{Equation 13}$$

The highest value of standard deviation occurs near the inflection of the conversion curve. At this point, in fact, the reaction is influenced both on a kinetic level, as the temperatures are not yet so high, and also on a diffusive level. A minimal variation in operating conditions determines a profound change in the conversion value. Despite this, it can be stated that the results differ by a maximum of

5% from each other. Obtaining similar conversions between the various tests guarantees the uniformity of the synthesized sample and the absence of contamination during the synthesis phase.

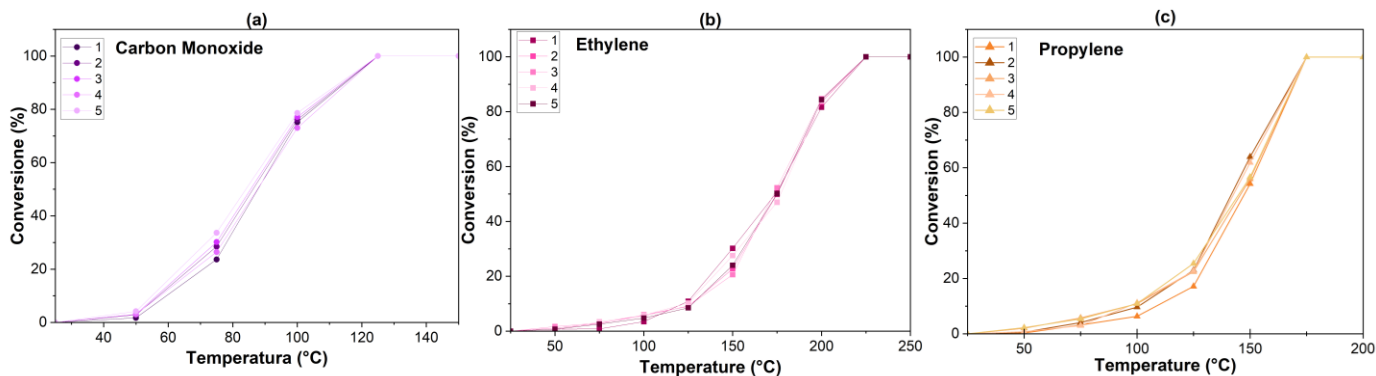


**Figure 6.7** (a), (b), (c) reproducibility tests in dry condition of Carbon monoxide, ethylene and propylene molecules

The highest value of standard deviation occurs near the inflection of the conversion curve. At this point, in fact, the reaction is influenced both on a kinetic level, as the temperatures are not yet so high, and on a diffusive level. A minimal variation in operating conditions determines a profound change in the conversion value. Despite this, it can be stated that the results differ by a maximum of 5% from each other. Obtaining similar conversions between the various tests guarantees the uniformity of the synthesized sample and the absence of contamination during the synthesis phase.

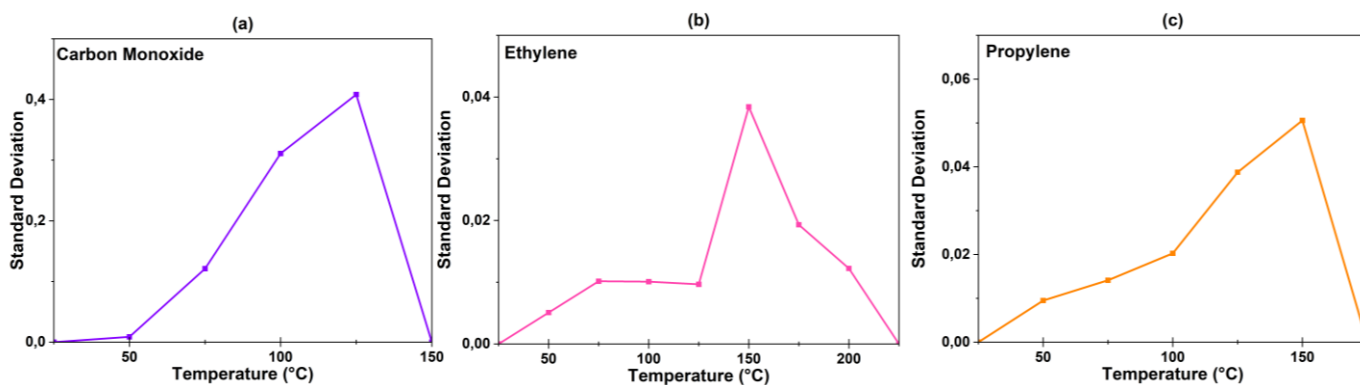


**Figure 6.8** (a), (b), (c) standard deviation results reproducibility tests of Carbon monoxide, ethylene and propylene molecules

## 7 Conclusions

The following thesis aimed to study manganese oxide-based catalysts regarding the reduction of toxic molecules present in indoor environments such as carbon monoxide, ethylene, and propylene. First, manganese oxides were found to be good catalysts for the reduction of these substances at temperatures below 300°C, especially MnO<sub>2</sub> SCS. A greater specific area and a smaller size of the crystallites allows for more active sites available for oxidation reactions. The activity of MnO<sub>2</sub> SCS as it has a higher percentage of Mn<sup>4+</sup> ions and O<sub>α</sub> on the surface compared to the other catalysts considered.

The presence of water affects the performance of MnO<sub>2</sub> SCS and there is an increase in temperature to achieve total conversion.

In the cyclic tests there was no change in conversion. TOS tests conducted in the absence of water demonstrated the stability of the fresh MnO<sub>2</sub> SCS catalyst. While as regards the sample already used for the cyclic tests, there was a slight drop in conversion in the last hours of testing, for the ethylene and propylene molecules probably due to a capping phenomenon of some active sites.

TOS in the presence of humidity have highlighted how the presence of water vapor slows down the arrival at a stationary conversion phase. The data can be considered reproducible thanks to the tests carried out in the last experimental phase.

In the future we could try to delve deeper into the topic linked to the degradation phenomena that predominantly influence the hydrocarbon molecules of ethylene and propylene. Furthermore, it would be interesting to analyze the behavior of the catalyst as the number of reaction cycles increases. In order to improve the performance of the catalyst, it would be advisable to add it with a noble metal such as gold or platinum in order to decrease the operating temperature.

## List of images

<b>Figure</b> 3.1 Physisorber of N <sub>2</sub>	51
<b>Figure</b> 4.1 Dry condition experimental system	56
<b>Figure</b> 4.2 Wet condition experimental system	57
<b>Figure</b> 4.3 Drexels	58
<b>Figure</b> 5.1 Physisorption of N <sub>2</sub> : MnO <sub>2</sub> , Mn <sub>2</sub> O <sub>3</sub> SCS, commercial	59
<b>Figure</b> 5.2 Pore size distribution of MnO <sub>2</sub> , Mn <sub>2</sub> O <sub>3</sub> SCS, commercial	60
<b>Figure</b> 5.3 Diffraction pattern of MnO <sub>2</sub> , Mn <sub>2</sub> O <sub>3</sub> SCS, commercial	60
<b>Figure</b> 5.4 Structure of MnO <sub>2</sub> , Mn <sub>2</sub> O <sub>3</sub> SCS on CAD	61
<b>Figure</b> 5.5 XPS Spectra of MnO <sub>2</sub> , Mn <sub>2</sub> O <sub>3</sub> SCS and commercial	62
<b>Figure</b> 5.6 H <sub>2</sub> -TPR profiles of MnO <sub>2</sub> , Mn <sub>2</sub> O <sub>3</sub> SCS	63
<b>Figure</b> 5.7 O <sub>2</sub> -TPD profiles of MnO <sub>2</sub> , Mn <sub>2</sub> O <sub>3</sub> SCS, commercial	63
<b>Figure</b> 5.8 FESEM catalysts SCS	63
<b>Figure</b> 6.1 Dry conditions tests with MnO <sub>2</sub> , Mn <sub>2</sub> O <sub>3</sub> SCS, commercial	64
<b>Figure</b> 6.2 Wet condition tests MnO <sub>2</sub> SCS	66
<b>Figure</b> 6.3 Cyclic tests dry condition MnO <sub>2</sub> SCS	68
<b>Figure</b> 6.4 TOS dry condition MnO <sub>2</sub> SCS fresh	68
<b>Figure</b> 6.5 TOS dry condition MnO <sub>2</sub> SCS non fresh	70
<b>Figure</b> 6.6 TOS wet condition MnO <sub>2</sub> SCS	70
<b>Figure</b> 6.7 Reproducibility tests MnO <sub>2</sub> SCS	71
<b>Figure</b> 6.8 Standard Deviation of samples MnO <sub>2</sub> SCS	73

## List of tables

-  
Tabella I ; 8  
Tabella II; 10  
Tabella III; 11  
Tabella IV; 11  
Tabella V; 13  
Tabella VI; 14  
Tabella VII; 16  
Tabella VIII; 17

-  
Table 1; 58  
Table 2; 59  
Table 3; 60  
Table 4;61  
Table 5; 61  
Table 6; 62  
Table 7;63  
Table 8;64  
Table 9;64  
Table 10;66  
Table 11;66  
Table 12 ;66  
Table 13 ;67  
Table 14;69  
Table 15 ;70  
Table 16;71  
Table 17;71

## List of equations

Equation 1  
Equation 2  
Equation 3  
Equation 4  
Equation 5  
Equation 6  
Equation 7  
Equation 8  
Equation 9  
Equation 10  
Equation 11

## Riferimenti

- A.Kopp Alves et al. (2013). Novel Synthesis and Characterization of Nanostructured Materials. *Springer-Verlag Berlin. Heidelberg*.
- al, K. e. (s.d.).
- Alain Manceau, A. I. (1992). Structural chemistry of Mn, Fe, Co, and Ni in manganese hydrous oxides: Part 1 information from XANES spectroscopy. In A. I. Alain Manceau, *American Mineralogist* (p. 11133-1143).
- Alexander S. Mukasyan, P. E. (2007). Solution combustion synthesis of nanomaterials. *Science Direct*, 1789-1795.
- Arvind Varma, A. S. (2016). Solution Combustion Synthesis of Nanoscale Materials. *Chemical review*, 14494-14552.
- Baldi, G. (s.d.). *Mio nonno in cariola*. Tratto da photometrics : [<https://photometrics.net/field-emission-scanning-electron-microscopy-fesem>]
- Bergefurt, L., Weijs-Perree, M., Appel-Meulenbroek, R., & Arentze, T. (2022). Bergefurt, L.; Weijs-Perree, M.; Appel-Meulenbroek, R.; Arentze, T. The physical office workplace as a resource for mental health-a systematic scoping review. *Build. Environ.* 2022, 207, 108505. . 207(208505).
- calculatona, F. (s.d.).
- Clarissa Cocuzza, E. S. (2023). M. J. Marin Figueredo et al., “Cerium–Copper–Manganese Oxides Synthesized via Solution. *Catalysis Today*.
- David A. Tompsett, S. C. (2014). Rutile ( $\beta$ -)MnO<sub>2</sub> Surfaces and Vacancy Formation for High. *Journal American Chemistry society JAC*, 13(dx.doi.org/10.1021/ja4092962), 1418–1426.
- Deng, S. K. (2016). Promotional effect of iron oxide on the catalytic properties of Fe–MnO<sub>x</sub>/TiO<sub>2</sub> (anatase) catalysts for the SCR reaction at low temperature. *Catalysis Science and technology*.
- EPA-452/F-03-022. (s.d.). Air Pollution Control Technology Fact Sheet.
- EPA's Terms of Environment Glossary, A. a. (s.d.). Code of Federal Regulations.
- Europe, W. H. (1989). *Indoor air quality and organic pollutants*. Berlin Meeting 23-27 August 1987.
- Fogler, S. (1999). “Elements of Chemical Reaction Engineering”. In *Third edition*. New Jersey. Prentice-Hall, Inc.
- Haibao Huang, Y. X. (2015). Low temperature catalytic oxidation of volatile organic compounds a review. *Catalysis and Science Technology*.
- Haibao Huang, Y. X. (2015). Low temperature catalytic oxidation of volatile organic compounds: a review. *Royal society of chemistry*, 5, 2649-2669.
- Hannah Blair, N. K. (2023). *Gli Effetti Invisibili della Cottura a Gas sulla salute*. CLASP.
- Hyun-Ha Kim, A. A. (2021). Interim report of plasma catalysis: Footprints in the past and blueprints for the future. *Plasma Environmental Science and Technology*, DOI: 10.34343/ijpest.2021.15.e01004.
- K. S. W. SING (UK, C., & al., D. H. (1982). “Reporting Physisorption Data for Gas/Solid Systems”. In *INTERNATIONAL UNION OF PURE AND APPLIED CHEMISTRY*. Great Britain .
- Katpteijin et al. (1994). *Appl Catalysis B Environmental*. In *Activity and selectivity of pure manganese oxides in the selective reduction of nitric oxide with ammonia* (p. 173-189). Amsterdam: Elsevier Science.
- Kaushik Natarajan, a. M. (2018). Visible light driven water splitting through an innovative Cu-treated-MnO<sub>2</sub> nanostructure: probing enhanced activity. *Royal Society of chemistry*.
- Laura Silvestri et al. (s.d.). *Caratterizzazione di materiali porosi* . Roma: ENEA – Unità Tecnica Tecnologie dei Materiali.

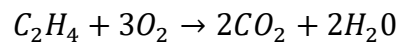
- Paul B. Tchounwou, A. E. (2021). Volatile Organic Compounds (VOCs) as Environmental Pollutants: Occurrence and Mitigation Using Nanomaterials. *Int J Environ Res Public Health*. .
- Pollution System*. (s.d.). Tratto da <https://www.pollutionsystems.com/air-pollution-systems/catalytic-oxidizers>
- Prasad, S. D. (2019). Advances in transition metal oxide catalysts for carbon monoxide oxidation a review. *Advanced Composites and Hybrid Materials* (, 626,656.
- Principali inquinanti indoor e loro fonti*. (2015). Tratto da Ministero della Salute: [https://www.salute.gov.it/portale/temi/p2\\_6.jsp?id=4389&area=indor&menu=vuoto](https://www.salute.gov.it/portale/temi/p2_6.jsp?id=4389&area=indor&menu=vuoto)
- R. Nikam, S. R. (2017). Structural and Magnetic Properties of Fe-Doped Mn<sub>2</sub>O<sub>3</sub> Orthorhombic Bicibiite. *Journall of supercapacitor and novel magnetism* , 2179-2185.
- Ray, S. a. (2011). Quantitative Analysis of Adsorbed Proteins by X-ray Photoelectron Spectroscopy. *Analytical Chemistry*, 8659-8666.
- review, C. o. (2022). Biyuan Liu. *Journal of Hazardous Materials*, 1268547.
- Sang Chai Kima, W. G. (2010). Catalytic combustion of VOCs over a series of manganese oxide catalysts. <http://www.elsevier.com/locate/apcatb>, <https://doi.org/10.1016/j.apcatb.2010.05.027>, 180-185.
- Satu Ojala, S. P. (2011). Catalysis in VOC Abatement. *Top Catalysis*(DOI 10.1007/s11244-011-9747-1), 1224-1256.
- Schweitzer, N. M. (2022). Induce to reproduce. *Q&A, Nature Catalysis* , 658-661.
- Siegbahn, K., & Edvarson. (s.d.). "β-Ray spectroscopy in the precision range of 1 : 10<sup>5</sup>". doi:10.1016/S0029-5582(56)80022-9.
- Sundell, J. (2004). On the history of indoor air quality and health. *Blackwell Munksgaard*, 51-58.
- SusannaH L. Scott, G. e. (2022). To err is Human; To reproduce takes time. *ACS Catalysis*, 3644-3650.
- Teresa Gelles, A. K. (2020). Abatement of gaseous volatile organic compounds: A material perspective. *Catalysis today*, 3-18.
- UNI EN ISO159, C. T. (2003). Ventilazione per edifici., (p. prEN 13779). Roma.
- V.P. Santos, M. P. (2010). The role of lattice oxygen on the activity of manganese oxides towards theoxidation of volatile organic compounds. *Applied Catalysis B Environmental*(99).
- Vedrine, J. C. (2019). Importance, features and uses of metal oxide catalysts in heterogeneous catalysis. *Science Direct*, 40([https://doi.org/10.1016/S1872-2067\(18\)63162-6](https://doi.org/10.1016/S1872-2067(18)63162-6)), 1627-1636.
- Wang, L. H. (2022). Building and Health: Mapping the Knowledge Development of Sick Building Syndrome. (308,22).
- Xueyang Zhang, e. a. (2017-09-15, september 15). Adsorption of VOCs onto engineered carbon materials: A review. *Journal of Hazardous Materials*, 102-123, <https://doi.org/10.1016/j.jhazmat.2017.05.013>.
- Yunlong Guo, M. W. (2021). Recent advances in VOC elimination by catalytic oxidation technology onto nanoparticles catalysts: a critical review. *Applied Catalysis B: Environmental*, 119447.
- Yunlong Guo, M. W. (2021). Recent advances in VOC elimination by catalytic oxidation technology onto nanoparticles catalysts: a critical review. *Environmental Catalysis B*, 22290(119447). doi:<https://doi.org/10.1016/j.apcatb.2020.119447>
- Z. Zhang, e. a. (2015). Low-temperature catalysis for VOCs removal in technology and application: A state-of-the-art review.
- Zeesham Ajmal, M. u. (2022, December). Recent advancement in conjugated polymers based photocatalytic technology for air pollutants abatement: Cases of CO<sub>2</sub>, NO<sub>x</sub>, and VOCs. *Chemosphere, volume 308, part 2*, p. <https://doi.org/10.1016/j.chemosphere.2022.136358>.
- Zhang, J. S. (2016). Low. temperature catalysis for VOCs removal in technology and application: A stet of the art review. *Catalysis Today* 264, 270-278.

# Appendix

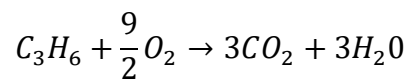
## List of formula

Reaction equation:

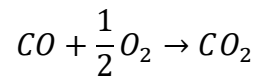
Ethylene



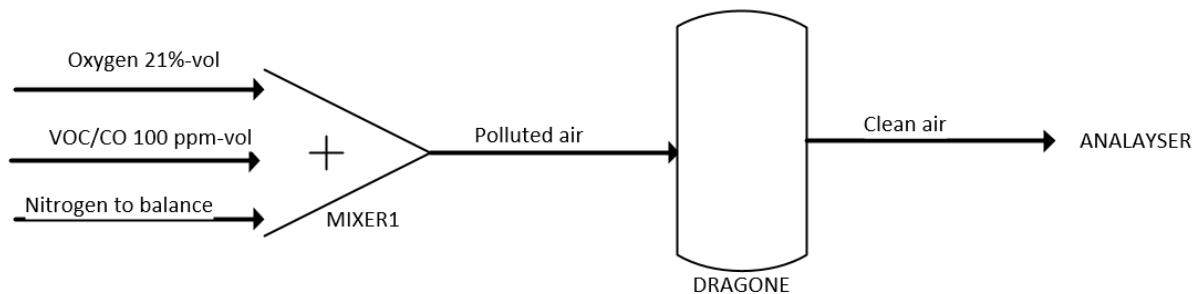
Propylene



Carbon Monoxide



Balance of inlet currents: the assigned experimental VOC cylinders were composed of 1000 ppm-vol of the substance of interest (Ethylene, Propylene, Carbon Monoxide) the remaining part was Nitrogen. Consequently, to insert the molar bearings, a budget had to be initially made:



Since the total volume flowrate entering in the reactor must be equal to 50 ml/min, in order to calculate the inlet composition of each component the following formula has been used:

$$V_{i,in} = V_{Tot,out} \frac{i_{\%out}}{i_{\%in}}$$

Where the symbols

$V_{i,in}$  is the volume flowrate at the inlet of each component.

$V_{Tot,out}$  is the volume flowrate total at the outlet.

$i_{\%out}$  volume percentage at the outlet of i-component

$i_{\%in}$  volume percentage at the inlet of i-component



Propylene (1003 ppm in Nitrogen)

Inlet composition				
-	%	%	%	ml/min
Oxygen	100%	-	21%	10,5
Propylene	-	10%	0,01%	5,015
Nitrogen	-	90%	78,99%	34,45

Ethylene (1000 ppm in Nitrogen)

Inlet composition				
-	%	%	%	ml/min
Oxygen	100%	-	21%	10,5
Ethylene	-	10%	0,01%	4,5
Nitrogen	-	90%	78,99%	35

Carbon monoxide (1115 ppm in Nitrogen)

Inlet composition				
-	%	%	%	ml/min
Oxygen	100%	-	21%	10,5
Carbon Monoxide	-	10%	0,01%	5
Nitrogen	-	90%	78,99%	34,5

## Acronyms List

<b>FESEM</b>	<b>Field Emission Scanning Electron Microscope</b>
<b>TPD</b>	Temperature programmed desorption
<b>TPR</b>	Temperature programmed reduction
<b>XPS</b>	X-ray photoelectron spectroscopy
<b>XRD</b>	W-ray diffraction
<b>BET</b>	Brauner Emmett Teller
<b>SCS</b>	Solution Combustion Synthesis
<b>Comm</b>	commercial
<b>VOC</b>	volatile organic compound
<b>SVOC</b>	semi volatile organic compound
<b>OVOCs</b>	Oxygenated Volatile compounds
<b>VVOC</b>	Very volatile organic compound
<b>TOS</b>	time on stream
<b>WHO</b>	World Health Organization
<b>SBS</b>	Sick Building Syndrome
<b>CLASP</b>	
<b>TC</b>	technical council
<b>IDA-C</b>	internal air control system
<b>EHA</b>	exhausted air
<b>ETA</b>	extracted air
<b>ODA</b>	external air
<b>IDA</b>	internal air control system
<b>SUP</b>	supply air
<b>ACFs</b>	activated carbon fibers
<b>CNTs</b>	carbon nanotubes
<b>CSCs</b>	carbon - silica composites
<b>CCMs</b>	cryogels microspheres
<b>CPs</b>	conjugated polymers
<b>IAD</b>	internal air quality
<b>PCO</b>	photocatalytic oxidation
<b>ETS</b>	Tobacco Smoke
<b>PM</b>	particulate Matter
<b>TLV</b>	Threshold Limit Value
<b>ARI</b>	respiratory infections
<b>MCS</b>	multiple chemical sensitivity
<b>BTX</b>	Benzene Toluene Xylene
<b>BE</b>	Binding energy
<b>SHS</b>	Self-propagating high temperature synthesis
<b>CS</b>	Combustion Synthesis

## Ringraziamenti

Finalmente dopo cinque anni sono felice di ringraziare i miei genitori che mi hanno dato la possibilità di intraprendere questa strada, senza il loro appoggio non sarebbe stato possibile arrivare fino a qui. Grazie a mamma, per avermi insegnato cosa vuol dire non mollare mai e per essermi sempre stata uno “squillo di chiamata” distante. Grazie a mio papà, per avermi dimostrato che la disciplina e la costanza pagano sempre.

Un grazie particolare a Mati la migliore coinquilina di sempre e Ana che, anche se lontana, mi è sempre rimasta vicina. Si sono dimostrate le sorelle migliori che potessi mai desiderare.

Voglio ringraziare anche i miei compagni di “viaggio”, con cui ho costruito un rapporto speciale e unico. Siete stati una parte fondamentale della mia vita universitaria per i momenti indimenticabili che abbiamo vissuto insieme. Citazioni doverose a Lorenzo per quel pomeriggio domenicale e ad Albe che con il suo ottimismo mi ha permesso di finire gli esami a luglio.

Infine, un sentito ringraziamento va a Nadia che mi ha seguito, con pazienza e gentilezza, in ogni singolo passo di questo ultimo progetto.